The Cerebellum (2021) 20:631–658
https://doi.org/10.1007/s12311-020-01224-5

REVIEW

Diagnostic Approach to Cerebellar Hypoplasia

Andrea Accogli [1,2,3] · Nassima Addour-Boudrahem [4] · Myriam Srour [1,4,5,6]

Accepted: 2 December 2020 / Published online: 3 February 2021

Abstract

Cerebellar hypoplasia (CH) refers to a cerebellum of reduced volume with preserved shape. CH is associated with a broad heterogeneity in neuroradiologic features, etiologies, clinical characteristics, and neurodevelopmental outcomes, challenging physicians evaluating children with CH. Traditionally, neuroimaging has been a key tool to categorize CH based on the pattern of cerebellar involvement (e.g., hypoplasia of cerebellar vermis only vs. hypoplasia of both the vermis and cerebellar hemispheres) and the presence of associated brainstem and cerebral anomalies. With the advances in genetic technologies of the recent decade, many novel CH genes have been identified, and consequently, a constant updating of the literature and revision of the classification of cerebellar malformations are needed. Here, we review the current literature on CH. We propose a systematic approach to recognize specific neuroimaging patterns associated with CH, based on whether the CH is isolated or associated with posterior cerebrospinal fluid anomalies, specific brainstem or cerebellar malformations, brainstem hypoplasia with or without cortical migration anomalies, or dysplasia. The CH radiologic pattern and clinical assessment will allow the clinician to guide his investigations and genetic testing, give a more precise diagnosis, screen for associated comorbidities, and improve prognostication of associated neurodevelopmental outcomes.

Keywords Cerebellar hypoplasia · Vermis hypoplasia · Pontocerebellar hypoplasia · Molar tooth sign · Rhombencephalosynapsis · Diagnostic approach · Cerebellar dysplasia · Genetics of cerebellum

Introduction

The cerebellum accounts for only about 10% of the cerebral volume (hence the name of "little brain") but contains approximately half of the 50 billion mature neurons of the adult brain [1]. Beyond the well-known role of cerebellum in motor coordination, an expanding literature has recognized the role of different cerebellar subregions in many neurocognitive functions, such as language and behavior [2, 3], suggesting that the impairment of specific cerebro-cerebellar circuits is relevant to the development of several neurodevelopmental disorders like autism spectrum disorder (ASD) [4], language disorders [5], and attention deficit and hyperactivity (ADHD) [6].

The term cerebellar hypoplasia (CH) refers to a "cerebellum of reduced volume." It encompasses an extremely heterogeneous group of disorders possessing a wide range of radiologic features, variable clinical characteristics and neurodevelopmental outcomes, and diverse acquired and genetic etiologies [7]. Over the past years, various neuroradiological approaches have been proposed to classify CH and related anomalies but an unanimous consensus has not been attained, given the heterogeneous and overlapping phenotypic spectrum among the CH-related disorders [8–12]. Here, we review the current literature related to CH and propose a systematic diagnostic approach for clinicians evaluating patients with cerebellar malformations.

We conducted a search of the PubMEd database from January 1990 to October 2020, using the terms "cerebellar

✉ Myriam Srour
myriam.srour@mcgill.ca

1 Department of Pediatrics, Division of Pediatric Neurology, McGill University, Montreal, Canada

2 Unit of Medical Genetics, IRCCS Istituto Giannina Gaslini, Genoa, Italy

3 Department of Neurosciences, Rehabilitation, Ophthalmology, Genetics, Maternal and Child Health (DINOGMI), University of Genoa, Genoa, Italy

4 McGill University Health Center (MUHC) Research Institute, Montreal, Canada

5 Montreal Neurological Institute, McGill University, Montreal, Canada

6 Departments of Pediatrics, Neurology & Neurosurgery, McGill University, MUHC-Research Institute, 1001 Blvd Décarie, Montreal H4A 3J1, Canada

development," "cerebellar hypoplasia," "cerebellar dysplasia," "posterior fossa malformation," "Dandy walker malformation," and "pontocerebellar hypoplasia." Additional references that were cited in relevant articles were also used.

Overview of Cerebellar Anatomy and Embryology

The cerebellum consists of two hemispheres and a midline vermis that are divided into 3 lobes and 10 lobules [13] (Fig. 1a). The cortex is three-layered and formed by the internal granule cell, Purkinje cell, and molecular layers (Fig. 1c). The excitatory glutaminergic granule cells receive inputs from outside the cerebellum and project onto the inhibitory GABAergic Purkinje cells. The Purkinje cells then project to cerebellar nuclei, which in turn connect directly or indirectly to the brainstem, spine, and diverse cerebral subcortical and cortical regions [14] (Fig. 1b). The molecular layer, in which granule cell axons and Purkinje dendrites interact, also contains stellate and basket cells [15].

Human cerebellar development begins around the ninth week of gestation and follows highly orchestrated processes that are critical between 20 and 40 weeks of gestation and continue postnatally [2, 16]. The cerebellum develops from the dorsal aspect of the rhombencephalon, at the level of the fourth ventricle. The rhombic lip, a thin strip of neuroepithelium that borders the fourth ventricle roof plate, gives rise to all the glutaminergic neurons (including granule cells and cerebellar nuclei neurons), whereas the ventricular zone gives rise to the GABAergic neurons (including the Purkinje cells).

Several transcription factors, such as Atoh1 and Pax6 in the rhombic lip and external germinal layer, and Ptf1a in the ventricular neuroepithelium, determine the spatio-temporal expression of cerebellar neuron progenitors during early development [17, 18]. The proliferation of the granule cells, which constitute the most abundant neurons in cerebellar neuronal circuitry, is critically dependent on the secretion of Sonic hedgehog (SHH) by the Purkinje cells [19], while their switch from proliferation to differentiation is tightly regulated by Notch and Wnt signalling [20]. Toward the end of the

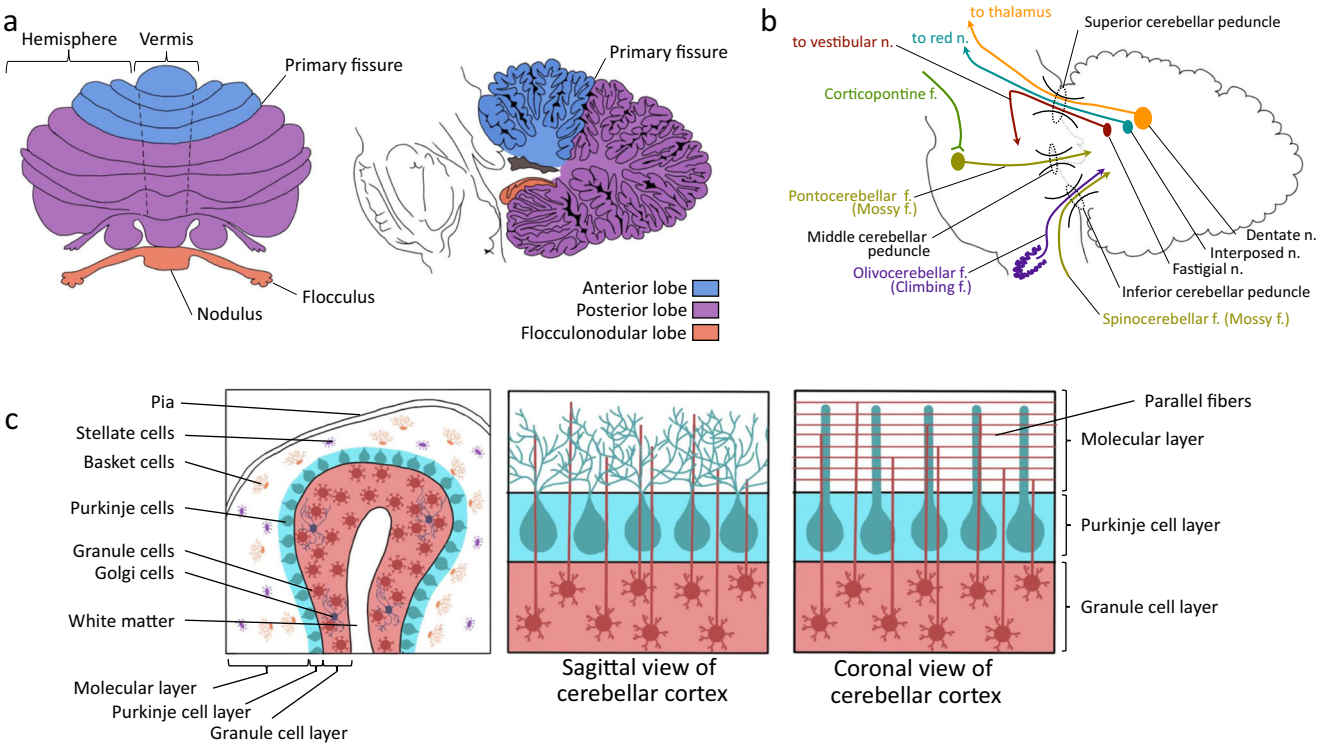

Fig. 1 Depiction of cerebellar anatomy. **a** The cerebellum is formed of 3 lobes (anterior, posterior, and flocculonodular) and 10 lobules, and is divided into a midline vermis and two hemispheres. **b** The inferior and middle cerebellar peduncles carry the main inputs to the cerebellum: (i) the pontocerebellar and spinocerebellar fibers that form the mossy fibers which synapse onto the granule cells, and (ii) the olivocerebellar fibers which form the climbing fibers and synapse onto the Purkinje cells. All the outputs from the cerebellum are relayed by the three cerebellar nuclei (dentate, interposed, and fastigial) and are carried by the superior cerebellar peduncle. **c** The cerebellar cortex is formed of three layers: the molecular layer, Purkinje cell layer, and granule cell layer. The excitatory glutaminergic granule cells receive inputs from outside the cerebellum and project their specialized axonal parallel fibers onto the dendrites of the inhibitory GABAergic Purkinje cells in the molecular layer. The Purkinje cells then project to cerebellar nuclei, which in turn connect directly or indirectly to the brainstem, spine, and diverse cerebral subcortical and cortical regions

embryonic period, granule cell precursors have migrated from the rhombic lip, reaching the superficial part of the cerebellum, the external germinal layer [21].

The fetal cerebellum can be detected by maternal transabdominal ultrasound as early as 12–13 weeks of gestation. Starting at 18 to 20 weeks of gestation, prenatal fetal magnetic resonance imaging (MRI) can reliably depict fetal cerebellar anatomy. The vermis can be clearly visualized by 15 weeks and the primary fissure at 18–20 weeks. After 21 weeks, the posterior fossa structures are well defined [22]. Increase in size of the vermis is more rapid in the third trimester, while the cerebellar hemispheres have a more rapid growth after birth [22].

Approach to Cerebellar Hypoplasias

Traditionally, the diagnosis of cerebellar hypoplasia has relied on the subjective evaluation of neuroradiologists who identify either an isolated small vermis or an overall reduced volume of cerebellum in comparison with brainstem and other brain structures. Recently, reference biometric data of vermis and brainstem have been provided, by studying a large cohort of about 700 children with normal cerebellum [23]. However, the relevance of these 2D measurements needs to be further validated in diseases presenting with cerebellar abnormalities.

One of the first crucial steps when considering a small cerebellum on imaging is to distinguish between hypoplasia and atrophy, given the significant differences in terms of clinical presentation, prognosis, and diagnostic work-up. CH refers to a cerebellum of a reduced volume, but with a normal or near-normal shape with normal interfoliate fissures and sulci [24, 25] (Fig. 2A–C). On the other hand, cerebellar atrophy implies a progressive loss of cerebellar parenchyma with secondary enlargement of the interfolial spaces and an increase in the size of the fourth ventricle [9] (Fig. 2D, D'). Distinguishing between cerebellar hypoplasia and atrophy is not always straightforward, especially if follow-up imaging is not available to document progressive changes. Some other neuroimaging clues, such as the presence of abnormalities of the cerebral cortex (such as polymicrogyria) or basal ganglia, are suggestive of a malformative process associated with cerebellar hypoplasia, whereas presence of signal abnormalities of the cerebellum or the cerebral white matter is suggestive of a metabolic process associated with cerebellar atrophy [25]. Cerebellar atrophy is not the subject of the current manuscript, deserving an extensive and specific diagnostic approach. The only group of disorders with cerebellar atrophy that we discuss is pontocerebellar hypoplasia (PCH) that, despite its name, includes a heterogeneous group of disorders with pontine and cerebellar hypoplasia and atrophy.

Once a radiologic diagnosis of cerebellar hypoplasia is made, the clinician will have to try to establish whether the hypoplasia is primary (i.e., developmental, genetic) or secondary (disruptive, acquired) [26] based on radiologic and clinical features. Acquired causes of cerebellar hypoplasia include prematurity, perinatal hypoxia, hemorrhage, prenatal infections, and exposure to teratogens. Therefore, a detailed prenatal and perinatal history should be obtained with particular attention for the evidence of low birth weight, intubation, hypotension, and sepsis in the neonatal period [9, 11, 27, 28]. Clues on imaging that suggest an acquired/disruptive cause include unilateral or asymmetric neuroradiological findings, evidence of hemorrhage or stroke, presence of cerebellar clefts, or posterior cerebral nodular heterotopias (Fig. 2E) [29]. Inclusion of iron-sensitive imaging sequences with 3T MRI in preterm infants enables the identification of hemorrhages as small as 2 mm which would provide evidence for an acquired, non-genetic cause of cerebellar hypoplasia [30]. Note that genetic conditions may also lead to predispositions to acquired cerebellar disruptions, such as dominant mutations in *COL4A1* which lead to change of the basal membrane of capillaries resulting in microangiopathy and predisposition to hemorrhage. Furthermore, cerebellar hypoplasia has been reported in up to a fourth of subjects with PHACE syndrome, a clinically recognizable neurocutaneous disorder characterized by posterior fossa anomalies, hemangioma, arterial anomalies, cardiac abnormalities/aortic coarctation, and eye abnormalities [31]. Unilateral cerebellar hypoplasia along with an ipsilateral posterior fossa cyst communicating with an asymmetrically distended 4th ventricle may be a clue for the prenatal diagnosis of PHACE syndrome [32, 33]. Specifically, "a tilted telephone receiver sign," consisting of upwardly rotated and deviated vermis merged with the contralateral cerebellar peduncles forming an elongated oblique connection between the cerebellar hemispheres on the coronal plane, has been suggested as a prenatal hallmark of PHACE syndrome [33].

Classifying cerebellar hypoplasias through recognition of neuroradiological patterns is essential in guiding investigations, establishing a specific diagnosis, and prognosticating possible neurodevelopmental outcomes. A diagnostic algorithm to CH is illustrated in Fig. 3. CH can be divided into six different subgroups, based on the type and location of associated neuroradiological anomalies (Table 1): [1] isolated vermis hypoplasia (VH)/CH, i.e., without any additional neuroradiologic anomalies; [2] VH/CH with posterior fossa cerebrospinal fluid (CSF) anomalies; [3] VH/CH with specific brainstem or cerebellar malformation (e.g., molar tooth sign); [4] VH/CH with brainstem hypoplasia; [5] VH/CH with brainstem and cortical migration anomalies; and [6] CH with cerebellar dysplasia (CD).

Isolated Vermis Hypoplasia and Cerebellar Hypoplasia

VH refers to a decreased volume of the vermis sparing the cerebellar hemispheres (Fig. 2B), whereas CH implies that

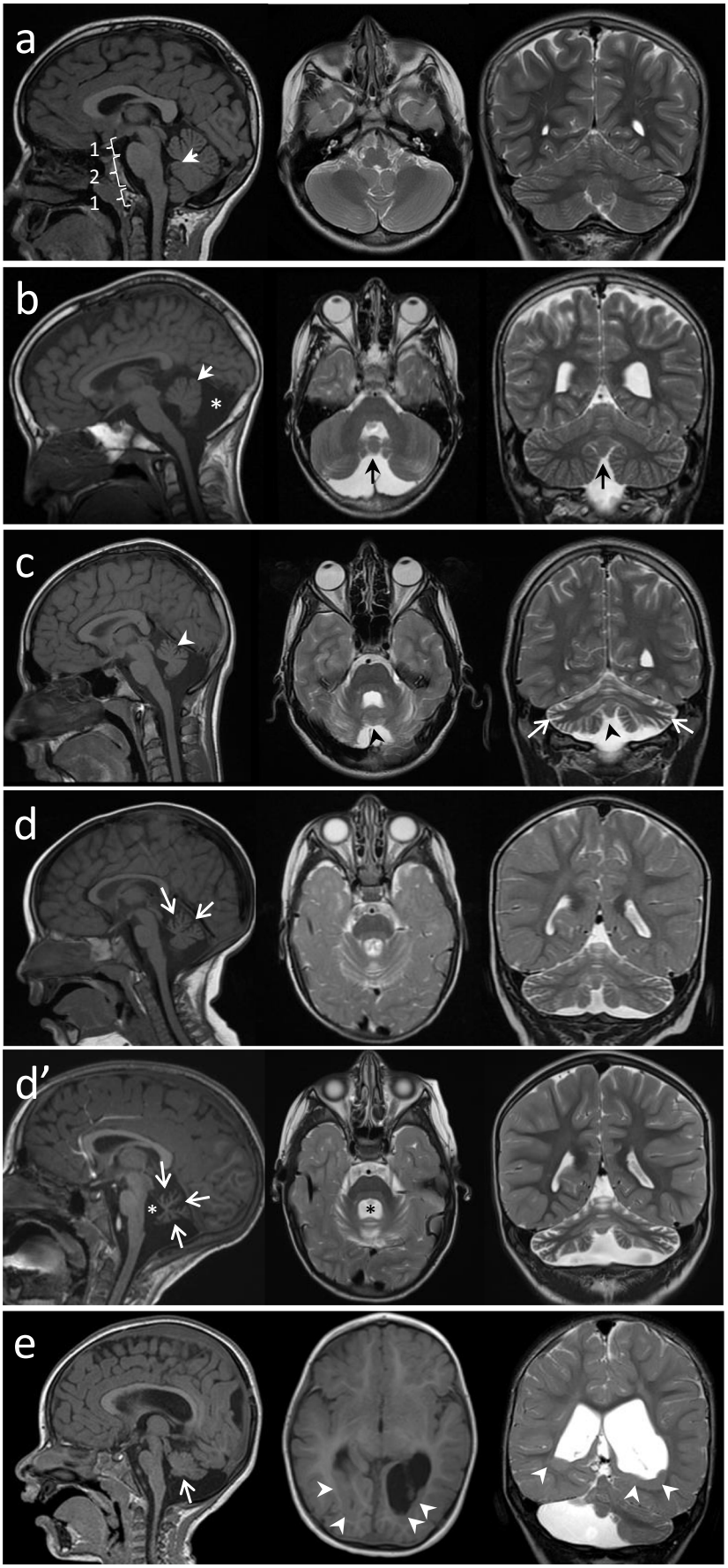
a
1
2
1
b
*
c
d
d'
*
e

◀ **Fig. 2** Radiologic patterns of cerebellar anomalies. A Normal cerebellum. Brain MRI showing a normal posterior fossa, brainstem, and cerebellum. On midsagittal section, the rostrocaudal length ratio of the midbrain:pons:medulla is 1:2:1, the dorsal surface of the brainstem is flat, and the position of the fastigium (arrowhead) is just below the midpoint of the ventral pons. The axial images show normal orientation of the cerebellar folia, running parallel to the calvaria. B Isolated cerebellar vermis hypoplasia. The vermis is of reduced volume (arrow) but of normal shape. Cisterns (asterisk) are prominent, but interfoliate fissures are normally spaced. The cerebellar hemispheres are normal. C Cerebellar vermis and hemisphere hypoplasia. A patient with CDG1a showing equal involvement of vermis (arrowhead) and hemispheres (arrows). D, D' Progressive cerebellar atrophy. MRI at 13 months (D) shows a cerebellum of normal shape, but increased space between the foliate fissures best noted on sagittal section (arrows). Progressive atrophy of the cerebellar vermis and hemispheres is noted on follow-up MRI at 4 years of age (D') with secondary enlargement of interfolial spaces and increase in the size of the fourth ventricle (asterisk). E Disruptive pattern of cerebellar hypoplasia. Cerebellar vermis hypoplasia involving especially the inferior vermis (arrow), and severe unilateral hypoplasia of the right cerebellar hemisphere. There is asymmetry of the cerebral ventricles with bilateral posterior periventricular heterotopias (arrowheads). The constellation of asymmetric findings in the cerebellum and posterior cerebral nodular heterotopias strongly suggests a prenatal disruptive/ischemic etiology

both vermis and hemispheres are involved with a possible variable gradient of severity (Fig. 2C). Isolated VH/CH refers to presence of vermis or cerebellum hypoplasia in the absence of other CNS radiological abnormality (i.e., normal brainstem and supratentorial structures). Dysmorphic features and extraneural congenital malformations, however, may be present.

Clinical features associated with isolated VH and CH are variable and may include hypotonia, truncal, appendicular and gait ataxia, and eye movement abnormalities (saccadic pursuit, nystagmus, oculomotor apraxia). The neurodevelopmental outcome of individuals with isolated VH or CH is extremely variable; however, CH is consistently associated with more severe motor and cognitive impairments and additional comorbidities [34, 35]. A recent study revealed that though some individuals with VH had normal intelligence, the majority had global developmental delay, and almost all had language delay though were verbal [35]. In contrast, all individuals with isolated CH had global developmental delay (mainly severe), with the majority being unable to ambulate independently, and almost half having severe intellectual disability [35].

Isolated VH and CH may be a feature of syndromic and non-syndromic intellectual disability and are associated with various chromosomal aberrations and monogenetic disorders. A dysmorphological assessment is crucial for diagnosis of an underlying syndrome displaying VH/CH. For example, VH/CH is a constant hallmark in CHARGE syndrome (MIM 214800), X-linked mental retardation with cerebellar hypoplasia, and distinctive facial appearance (MIM 300486) due to mutations in *OPHN1*, Galloway–Mowat syndrome 1 (MIM 251300), MARCH syndrome (MIM 236500) associated with bi-allelic *CEP55* mutations [36], and *WDR37*-associated disorder presenting with global developmental delay and/or intellectual disability, epilepsy, CH, coloboma, and facial dysmorphisms reminiscent of CHARGE syndrome [37].

Recent studies have revealed a high detection rate of clinically significant copy number variants (CNVs) in fetuses with CH (19.6–54.6%) and VH (6.5–33.3%) [38–40]. Examples include chromosome 2p15p16.1 deletion (due to *BCL11A* haploinsufficiency) [41], 5p15.33 microdeletions (Cri-du-chat syndrome), 6q27 terminal deletions, and Xq28 microduplications [38–40]. The diagnostic yield of chromosomal microarray is significantly higher in the presence of associated additional malformations [38]. Based on the current literature, chromosomal microarray analysis should be offered to all VH/CH individuals. Moreover, an intellectual disability gene panel, or when available whole-exome or -genome sequencing (WES, WGS), should be offered to VH/CH individuals presenting with intellectual disability, since VH/CH may be a non-specific finding in intellectual disability (ID) disorders [29]. A WES study in a large cohort of individuals with cerebellar malformations elucidated an underlying genetic cause in 51% of the CH cases [29]. Of note, the diagnostic yield was highest among individuals with CH who lacked prenatal risk factors (46%) and significantly lower in individuals with any prenatal risk factors (5%), underscoring the importance of a careful review of the medical history before pursuing genetic testing [29].

VH/CH and Posterior Fossa CSF Anomalies

Dandy–Walker Malformation

Dandy–Walker malformation (DWM, MIM 220200) is a heterogeneous disorder neuroradiologically defined by a hypoplastic, upwardly rotated vermis and dilatation of the fourth ventricle, resulting in a cystic appearance that may fill most of the posterior fossa (Fig. 5a). Consequently, the tentorium, torcular herophili, and transverse sinuses appear elevated [27]. The cerebellar hemispheres are typically hypoplastic and displaced anterolaterally. The main associated clinical feature is hydrocephalus, detected in up to 90% of individuals during infancy [42]. Additional cerebral malformations such as agenesis/hypoplasia of corpus callosum, polymicrogyria, nodular heterotopias, and occipital encephalocele are reported in up to 50% of patients [27].

DWM can be distinguished from other cystic posterior fossa malformations, such as Blake pouch cyst, posterior fossa arachnoid cyst, and mega cisterna magna. Blake pouch cyst consists of a retrocerebellar or infraretrocerebellar cyst that directly communicates with the fourth ventricle and can result in obstruction of CSF flow and tetraventricular hydrocephalus. Blake pouch cyst is thought to arise from failure of regression of Blake's pouch, the rudimental fourth ventricular tela

Table 1 Summary of imaging, clinical, and genetic characteristics of cerebellar hypoplasia and related anomalies

Cerebellar subgroup	Disorder	Neuroimaging features	Clinical features	Testing and associated genes	Inheritance
Isolated VH/CH	Very heterogeneous. Can be isolated VH/CH or part of syndromes/ID disorders.	VH with possible CHH, without any additional brain MRI findings.	VH often asymptomatic, > neurological signs and comorbidities in CH (e.g., DD, hypotonia, ataxia, nystagmus, possible dysmorphisms).	Array-CGH, targeted genetic testing for syndromic cases, ID panel, or WES if associated ID.	Sporadic, AD, AR, X-linked.
Posterior fossa CSF anomalies with or without VH/CH	Dandy–Walker malformation	Hypoplastic and upwardly rotated vermis, dilatation of the fourth ventricle. Possible additional features: hydrocephalus, CHH, CC anomalies, PMG, NH, holoprosencephaly (*ZIC2*), occipital encephalocele (*NID1*, *LAMC1*), cerebral small-vessel disease (*FOXC1*).	Macrocephaly due to hydrocephalus. Variable NDO. Axenfeld–Rieger syndrome (*FOXC1*), Ritscher–Schinzel/3C syndrome (*CCDC22*), intellectual disability (*CIP2A*).	*ZIC1/ZIC4* deletions (rare), *ZIC2/ZIC5* deletion (rare), *FOXC1* mutation/deletion, *NID1*, *LAMC1* and *CIP2A* mutations, *FGF17* deletion (rare), *CCDC22* mutation.	Sporadic (recurrence risk <5%) AD (*FOXC1*, *NID1*, *LAMC1*, *CIP2A*), X-linked (*CCDC22*).
	Blake pouch cyst (BPC)	Retrocerebellar/infraretrocerebellar cyst that communicates with the fourth ventricle, resulting in tetraventricular hydrocephalus. Normal cerebellum could be compressed, then re-expand after ventricular shunting.	Macrocephaly due to hydrocephalus.	None.	
	Posterior fossa arachnoid cyst (PFAC)	Well-circumscribed extra-axial fluid collection in the posterior fossa. Usually normal cerebellum.	Often incidental findings, asymptomatic.	None.	
	Mega cisterna magna (MCM)	Enlarged cisterna magna (10-mm diameter on midsagittal images). Absent hydrocephalus. Usually normal cerebellum.	Often incidental findings, asymptomatic.	None.	
VH/CH with specific midbrain anomalies	Molar tooth sign (Joubert syndrome–related disorders)*	Hypoplastic/dysplastic vermis, long/thick/horizontal SCPs. Possible additional features: PMG, NH, CC hypoplasia/ACC, encephalocele/cephalocele.	Hypotonia, alternating apnea/tachypnea, OMA, ataxia. Variable NDO, usually moderate. Additional features: retinal dystrophy, coloboma, oral hamartomas, liver fibrosis, nephronophthisis, polydactyly.	*AHI1*, *ARL13B*, *ARMC9*, *B9D1*, *B9D2*, *C2CD3*, *CC2D2A*, *CELSR2*, *CPLANE1*, *CEP41*, *CEP104*, *CEP290*, *CSPP1*, *IFT172*, *INPP5E*, *KIAA0586*, *KIAA0556*,	AR, X-linked (*OFD1* only).

Table 1 (continued)

Cerebellar subgroup	Disorder	Neuroimaging features	Clinical features		Testing and associated genes	Inheritance
					KIAA0753, *KIF7*, *MKS1*, *NPHP1*, *OFD1*, *RPGRIP1L*, *SUFU*, *TCTN1*, *TCTN2*, *TCTN3*, *TMEM67*, *TMEM107*, *TMEM138*, *TMEM216*, *TMEM231*, *TMEM237*, *TTC21B*, *ZNF423*.	
	Rhombencephalosynapsis	Partial/complete absence of cerebellar vermis and fusion of hemispheres and the dentate nuclei. Possible additional features: hydrocephalus due to aqueductal stenosis, fused colliculi, midline fusion of the tectum, absence of septum pellucidum, CC anomalies, PMG, holoprosencephaly.	Typical figure-of-eight headshaking behavior. Very variable NDO. Possible macrocephaly due to hydrocephalus.	Isolated RES.	Unknown.	
				Gómez–López–Hernández syndrome.	Unknown.	
				VACTERL-H	*ZIC3*, *FANCB*.	X-linked (*ZIC3*, *FANCB*).
				CEBALID syndrome.	*MN1*	AD
	Pontine tegmental cap dysplasia	Absence of the ventral pontine prominence with vaulted pontine tegmentum ("cap"). "Beak-like" dorsal pons and kinked brainstem in most severe cases. Possible additional features: VH, hypoplastic ICPs/MCPs, MTS-like aspect of the pontomesencephalic junction, and absent inferior olivary prominence.	Multiple cranial nerve deficits. Very variable NDO (perinatal death→normal intelligence). Possible congenital heart, kidney, vertebral, and rib defects.		Unknown.	
	Brainstem disconnection	Sub(total) absence of a brainstem segment (rostral and caudal brainstem portions connected only by a	Hypotonia, respiratory insufficiency. Poor NDO (13/14 cases died during infancy).		Unknown.	

Table 1 (continued)

Cerebellar subgroup	Disorder		Neuroimaging features	Clinical features	Testing and associated genes	Inheritance
			thin cord of tissue). VH often associated.	Possible vertebral segmentation defects and hydronephrosis.		
	Diencephalic–mesencephalic junction dysplasia		Broad phenotypic spectrum at the DMJ: typical "butterfly-like" appearance (not in all patients) at DMJ due to midbrain ventral cleft and hypothalamic–mesencephalic fusion/incomplete thalamic–mesencephalic cleavage. Cerebellar anomalies: from VH to PCH. Possible additional features in PCDH12 spectrum: thin CC, punctate brain calcifications, congenital hydrocephalus, and white matter tract defects.	Broad phenotype. Progressive microcephaly, hypotonia, spasticity, movement disorders, epilepsy, severe DD, craniofacial dysmorphisms (in all *PCDH12*).	*PCDH12* Unknown.	AR
	Oculocerebrocutaneous syndrome		Cerebellar vermis agenesis, CHH, dysplastic tectum and a large posterior fossa cyst. Possible additional features: frontal predominant PMG, NH, agenesis of the corpus callosum, ventriculomegaly/hydrocephalus.	Orbital cysts, anophthalmia/microphthalmia, focal aplastic/hypoplastic skin defects, and skin appendages.	Unknown.	
Cerebellar and brainstem hypoplasia	Pontocerebellar hypoplasia (PCH1–11)	PCH1	Hypoplastic cerebellum (VH = CHH) and pons (often mild and possible normal appearance at birth)	Spinal muscular atrophy, muscle weakness, decreased/absent reflexes, respiratory distress, congenital contractures.	*EXOSC3* (majority), *EXOSC8*, *TSEN54*, *VRK1*, *SLC25A46*	AR
		PCH2	Small pons and cerebellum with variable atrophy (CHH > VH results in "dragonfly" appearance), thin CC, possible cortical atrophy, and ventriculomegaly.	Severe progressive microcephaly, neonatal seizure, dyskinesia, chorea, spasticity, seizures, cortical visual impairment. Severe DD/poor NDO.	*TSEN54* (majority), *TSEN2*, *TSEN34*, *SEPSECS*, *VPS53.*	AR
		PCH3	Small pons and cerebellum (with atrophy), reduced	Hypotonia, hyperreflexia, seizure onset in infancy.	*PCLO*	AR

Table 1 (continued)

Cerebellar subgroup	Disorder	Neuroimaging features	Clinical features	Testing and associated genes	Inheritance
		cerebral white matter, optic atrophy.	Possible facial dysmorphisms. Severe DD/poor NDO		
	PCH 4/5	Severe pons and cerebellum hypoplasia (with atrophy).	Severe PCH2 phenotype. Poor NDO, often lethal in neonatal period.	*TSEN54*	AR
	PCH 6	Variable degree of pons and cerebellum hypoplasia (VH > CHH). Possible progressive supratentorial atrophy and increased lactate peak on MR spectroscopy.	Elevated CSF lactate (not all patients), epileptic encephalopathy (neonatal-early infancy onset). Cardiomyopathy and hydrops (1 patient), optic atrophy (1 patient). Severe DD.	*RARS2*	AR
	PCH7	Small cerebellum (with atrophy) and brainstem. Possible thin CC, ventriculomegaly.	Microcephaly, broad range of hypogonadism/ambiguous genitalia. Severe DD.	*TOE1*	
	PCH 8	Small pons and cerebellum (VH = CH) Possible thin CC.	Postnatal microcephaly, clubfoot/multiple joint contractures at birth, spasticity, ataxia; possible epilepsy and extrapyramidal movements. Severe DD, usually non-degenerative.	*CHMP1A*	AR
	PCH 9	Cerebellum (both vermis and hemispheres) and brainstem hypoplasia with "figure-of-8" appearance, thin CC/ACC. Possible hypomyelination, ventricular dilatation and cortical atrophy.	Progressive microcephaly (postnatal), spasticity, seizure onset in infancy, visual impairment. Possible dental anomalies and neuropathy age-dependent. Severe DD.	*AMPD2*	AR
	PCH 10	VH, thin brainstem, short/thin CC, possible simplified gyral pattern (> anterior–temporal regions).	Progressive microcephaly and epilepsy. Possible facial dysmorphisms and axonal sensorimotor neuropathy. Severe DD and motor impairment.	*CLP1*	AR
	PCH 11	Small pons and cerebellum, thin CC/ACC.	Microcephaly (primary/secondary), possible facial dysmorphisms, severe DD. Non-degenerative.	*TBC1D23*	AR
	PCH 12?	Small pons and cerebellum, thin CC, enlarged ventricles, possible atrophy of caudate nuclei	Microcephaly (primary/secondary), severe DD, possible epilepsy, ataxia,	*MINPP1*	AR

Table 1 (continued)

Cerebellar subgroup	Disorder	Neuroimaging features	Clinical features	Testing and associated genes	Inheritance
		and putamen, and white matter changes.	stereotypies, micropenis, cataracts/blindness.		
	CASK-related PCH	Small pons and cerebellum (VH = CCH). Possible reduction of frontal gyri and cortical atrophy.	Typically females (rarely males), progressive microcephaly, epilepsy, variable hearing loss. Possible dysmorphisms and nystagmus in males. Severe DD.	*CASK*	X-linked
	Congenital disorders of glycosylation	Small pons and cerebellum with progressive atrophy. Possible cortical atrophy, ventricular dilatation, cerebellar cortical T2 hyperintensity.	Extremely variable phenotype: abnormal fat distribution, retinitis pigmentosa, failure to thrive, elevated transaminases, coagulopathy, hypothyroidism, hypogonadism, seizures, stroke-like episodes, ataxia. Mild to severe DD.	Transferrin glycosylation analysis, *PMM2*, *SRD5A3*, and other CDG (rare).	AR
	Cerebellofaciodental syndrome	VH, flat brainstem, thin CC, enlarged cisterna magna.	Dysmorphic facial features, dental anomalies (taurodontism), short stature, microcephaly, scoliosis. Mild to severe DD.	*BRF1*	AR
	Osteogenesis imperfecta, type XV	Small brainstem, midbrain and variable cerebellum anomalies: from normal to absent vermis (usually VH > CCH). Possible brainstem hypoplasia (especially the tectum).	Osteogenesis imperfecta, unilateral ptosis. Autism and seizures reported in some. Normal intelligence to severe DD.	*WNT1*	AR
PCH spectrum cortical migration anomalies	Tubulinopathies*	VH/VD with possible cysts, small pons, variable spectrum of cortical anomalies from PMG to lissencephaly, enlarged tectum, dysmorphic basal ganglia, thin/absent CC.	Usually severe DD. Cognitive and motor impairments usually correlate with severity of brain malformations.	*TUBA1A*, *TUBB2B*, *TUBB3*.	AD
	Mental retardation, X-linked 102 (tubulin-like phenotype)	Bilateral frontal and perisylvian PMG/dysgyria, CC hypodysgenesis, dysmorphic basal ganglia, incomplete	DD, ID, +/− microcephaly, +/− hyposmia, +/− visual impairments, +/− movement disorders, +/− congenital heart defects.	*DDX3X*	X-linked

Table 1 (continued)

Cerebellar subgroup	Disorder		Neuroimaging features	Clinical features	Testing and associated genes	Inheritance
			hippocampal rotation, pons hypoplasia, VH/CH.			
	RELN/VLDLR-related CH		PCH spectrum with cortical migration defects: *RELN*: VH, CCH with poor foliation, lissencephaly/pachygyria. *VLDLR*: VH > CHH (less severe than RELN), simplified cortical gyral pattern.	Severe DD in individuals with *RELN* mutations. Usually milder phenotype in *VLDLR* mutation spectrum.	*RELN*, *VLDLR*.	AR
	Cobblestone cerebral cortex disorders*	Dystroglycanopathies (Walker–Warburg syndrome, muscle–eye–brain disease, Fukuyama muscular dystrophy)	VH/CHH + subcortical cerebellar cysts, thin and kinked brainstem, large tectum, cobblestone cerebral cortex, lissencephaly, pachygyria and PMG, and abnormal myelination. Tectocerebellar dysraphia (*DAG1*).	Eye involvement (cataracts, glaucoma, microphthalmia, coloboma, high myopia), neonatal hypotonia, muscle involvement (variably increased CK), microcephaly. Severe DD in the most severe spectrum.	*FKRP*, *FKTN*, *GTDC2*, *ISPD*, *LARGE*, *POMGNT1*, *POMT*, *POMT1*, *POMT2*, *GMPPB*, *TMTC3*, *B3GALNT2*, *DAG1*.	AR
		GPR56-related cobblestone cortex	VH + cysts (superior vermis), pons hypoplasia (< affected than dystroglycanopathies), bilateral frontoparietal cobblestone cerebral cortex, myelination abnormalities, and variable CC anomalies.	Usually normal OFC, severe DD, epilepsy, ataxia, possible nystagmus/strabismus.	*ADGRG1*	AR
		COL3A1-related cobblestone cortex	VH, dysplastic cerebellar cortex with multiple cortical cysts (superior > inferior), brainstem hypoplasia, diffuse/frontal cobblestone cortex, and diffuse hypomyelination. Possible thick/thin CC, ventriculomegaly, and intracranial vessel anomalies.	Variable phenotype: vascular Ehlers–Danlos syndrome features. DD/normal intelligence, possible seizure.	*COL3A1*	AR
	Additional rare disorders	Lissencephaly 7 with cerebellar hypoplasia*	VH/CCH with possible dysplasia, small pons, lissencephaly, ACC.	Progressive microcephaly, neonatal refractory seizures, facial dysmorphisms, lymphedema,	*CDK5*	AR

Table 1 (continued)

Cerebellar subgroup	Disorder	Neuroimaging features	Clinical features	Testing and associated genes	Inheritance
			arthrogryposis. Severe DD/neonatal death.		
	Polymicrogyria, perisylvian, with cerebellar hypoplasia and arthrogryposis	VH, dysplastic dentate nuclei, pons hypoplasia (one case), perisylvian PMG.	Arthrogryposis (autopsy findings).	*PI4KA*	AR
	Cerebellar ataxia, mental retardation, and dysequilibrium syndrome 2	Variable range of severity. Normal cerebellum to severe PCH, simplified gyral pattern to severe lissencephaly. Thin CC, possible congenital hydrocephalus.	Usually moderate to profound DD. Ataxia, progressive microcephaly; possible spasticity, epilepsy, nystagmus, dyskinesia.	*WDR81*	AR
	Alkuraya–Kučinskas syndrome	Cerebellar hypoplasia/atrophy, brainstem dysgenesis/kinked brainstem, lissencephaly to simplified gyral pattern, possible ventriculomegaly, ACC/thin CC.	Broad phenotypic spectrum including arthrogryposis, ophthalmologic anomalies (blepharophimosis, microphthalmia, cataract), cardiac and genital malformations, syndactyly. Moderate–severe DD/neonatal death.	*KIAA1109*	AR
	Lissencephaly 9 with complex brainstem malformation*	Pachygyria/lissencephaly (posterior > anterior gradient), hypoplastic and dysplastic brainstem with a striking W-shaped malformation (caused by small or absent pontine crossing fibers), thin anterior commissure, variably short CC, and mild to moderate VH/CH hypoplasia.	DD, severe ID, hypotonia, +/− spasticity, epilepsy, normal OFC.	*MACF1*	AD
	Mega-corpus-callosum syndrome with cerebellar hypoplasia and cortical malformations	Corpus callosum hyperplasia, mild to moderate brainstem (mainly pons) hypoplasia, CH (vermis > hemisphere hypoplasia), brainstem (mainly the pons) hypoplasia, ventricular dilatation, wide range of cortical malformations (ranging from subtle dysgyria to a tubulin-like phenotype).	DD, variable ID severity, +/− epilepsy, normal OFC.	*MAST1*	AD

Table 1 (continued)

Cerebellar subgroup	Disorder	Neuroimaging features	Clinical features	Testing and associated genes	Inheritance
	Cortical dysplasia, complex, with other brain malformations 9	Pachygyria, CC hypodysgenesis, CH, brainstem hypoplasia (1 subject)	DD, severe ID, ASD, secondary microcephaly, epilepsy, spasticity, +/− ataxia.	*CTNNA2*	AR
Cerebellar dysplasia	Poretti–Boltshauser syndrome	Cerebellar (vermis + hemispheres) dysplasia with cysts, often VH.	Ataxia, head titubation, eye anomalies (myopia, large globes, retinopathy, retinal vascular defect). Variable DD.	LAMA1	AR
	Chudley–McCullough syndrome	Inferior cerebellar hemisphere dysplasia, possible inferior VH, partial/total ACC, interhemispheric cyst/quadrigeminal plate cistern cyst, frontal subcortical heterotopia, frontal PMG.	Hearing loss, possible ataxia. Mild DD.	*GPSM2*	AR
	Epileptic encephalopathy, early infantile, 66	VH, mega cisterna magna, retrocerebellar arachnoid cyst, cerebellar foliar distortion, +/− patulous foramen Magendie.	DD, ID, epilepsy, hypotonia, facial dysmorphisms, +/− nystagmus, hand stereotypies, genital anomalies, +/− hematological anomalies, +/− distal limb features.	*PACS2*	AD

*Cerebellar dysplasia may be a feature of these cerebellar malformations

ACC, agenesis of corpus callosum; *AD*, autosomal dominant; *AR*, autosomal recessive; *ASD*, autism spectrum disorder; *CC*, corpus callosum; *CH*, cerebellar hypoplasia; *CHH*, cerebellar hemisphere hypoplasia; *CK*, creatine kinase; *DD*, developmental delay; *DWM*, Dandy–Walker malformation; *ICPs*, inferior cerebellar peduncles; *ID*, intellectual disability; *OFC*, occipital frontal circumference; *OMA*, oculomotor apraxia; *MCPs*, middle cerebellar peduncles; *NDO*, neurodevelopmental outcome; *NH*, nodular heterotopia; *PCH*, pontocerebellar hypoplasia; *PMG*, polymicrogyria; *SCPs*, superior cerebellar peduncles; *VD*, vermis dysplasia; *VH*, vermis hypoplasia, *WES*, whole-exome sequencing

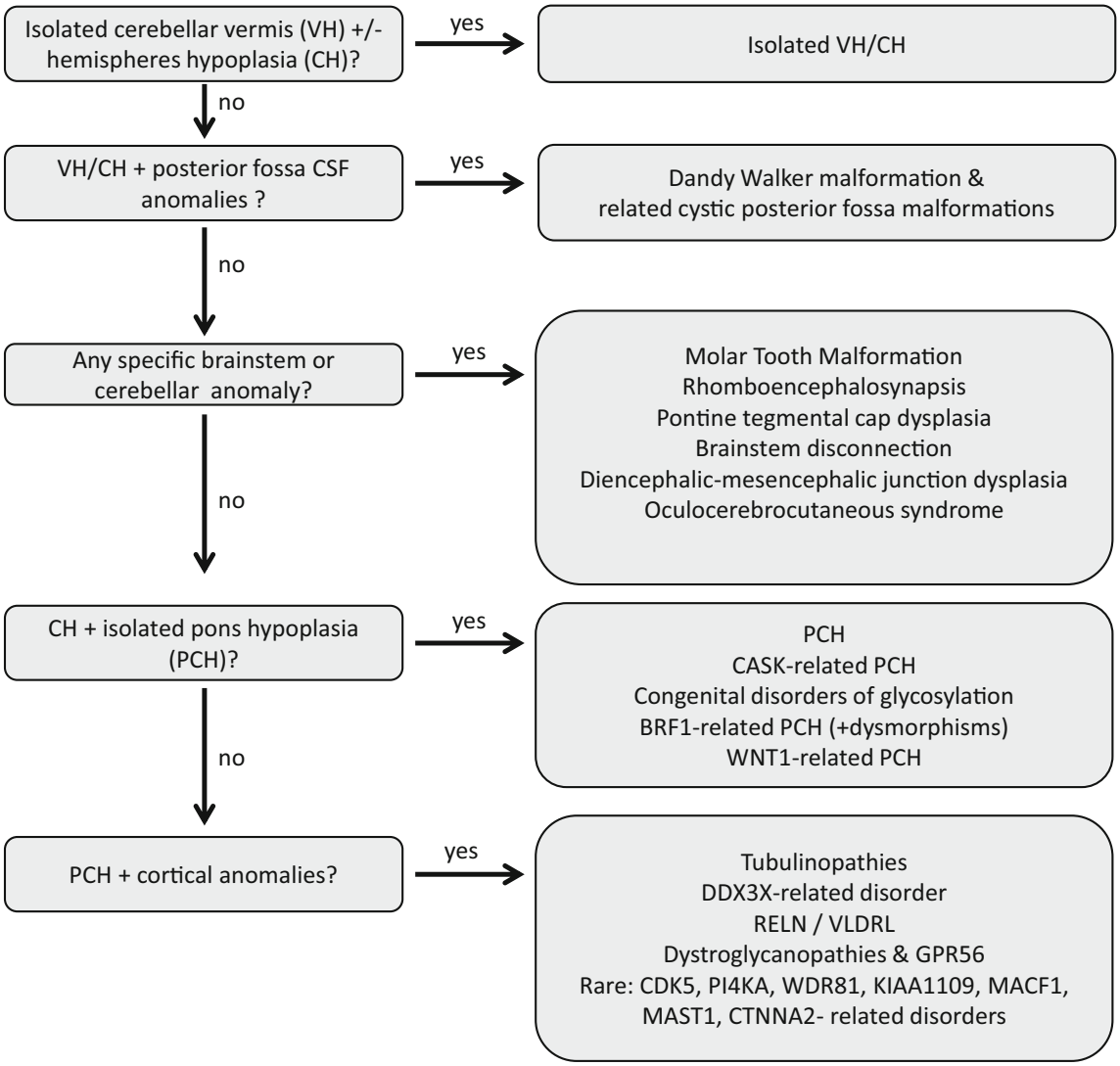

Fig. 3 Diagnostic algorithm of cerebellar hypoplasia and related anomalies. VH, vermis hypoplasia; CH, cerebellar hypoplasia; PCH, pontocerebellar hypoplasia; DWM, Dandy–Walker malformation

choroidea, secondary to nonperforation of the foramen of Magendie during development [43]. A posterior fossa arachnoid cyst is a well-circumscribed posterior fossa extra-axial fluid collection that can vary in terms of size and location (retrocerebellar, supravermian, anterior, or laterally to the cerebellar hemispheres) [27]. The posterior fossa arachnoid cyst may exert a mass effect on the normal cerebellum resulting in flattening of its curvature. Mega cisterna magna refers to an enlarged cisterna magna (10-mm diameter on midsagittal images) with a normal cerebellum and fourth ventricle. There is no associated hydrocephalus, as the mega cisterna magna freely communicates with the fourth ventricle and cervical subarachnoid spaces [27]. Mega cisterna magna and posterior fossa arachnoid cyst are often an incidental finding with an intact cerebellum and without clinical relevance.

Neurodevelopmental outcomes in DWM range from severe intellectual disability to completely normal development. DWM usually occurs sporadically with low risk of recurrence (1–5%) [44].

To date, only a few genes have been implicated in a minority of DWM cases. Heterozygous mutations in *FOXC1* are associated with DWM spectrum with white signal matter abnormalities [45]. *FOXC1* encodes a transcription factor that regulates neural crest cell development, playing a crucial role in multiple developmental processes of the posterior fossa mesenchyme, eye, cardiovascular system, and kidney [46]. Accordingly, *FOXC1* mutations account for a wide range of anomalies in addition to DWM and white matter hyperintensities, including typical eye anomalies of Axenfeld–Rieger syndrome (MIM 602482) and dilated perivascular spaces and cerebral small-vessel disease [47]. Interestingly, a genotype–phenotype correlation has been outlined in individuals carrying chromosome 6p25.3 deletions that encompass *FOXC1*, with a more severe DWM phenotype

in individuals with large 6p25.3 deletion and only VH in patients carrying small deletions [45].

DWM has been also described in individuals with 3q22.2–3q25.33 deletions that encompass *ZIC1* and *ZIC4* [48], two genes with an important role in cell proliferation and fate specification of the dorsal hindbrain [49]. In addition, several individuals with DWM and holoprosencephaly have been reported with 13q32.2–32.3 deletions encompassing *ZIC2* and *ZIC5* [50].

Recently, whole-exome sequencing has revealed pathogenic heterozygous mutations in *NID1* and its ligand *LAMC1* in two families with DWM and occipital encephalocele [51]. Furthermore, mutations in *CCDC22*, encoding a regulatory component of the NF-κb pathway, have been linked to X-linked intellectual disability with dysmorphic features and DWM (MIM 300963), overlapping with the phenotype of Ritscher–Schinzel syndrome (RSS)/3C (cranio-cerebro-cardiac) (MIM 220210), previously associated with DWM [52].

Lastly, *CIP2A*, a gene encoding an oncoprotein promoting tumor survival via inhibition of protein phosphatase 2A (PP2A), represents a novel candidate gene for DWM. A gain-of-function missense variant has been shown to increase the PP2A, mTOR, and c-Myc protein levels in peripheral blood mononuclear cells from two siblings with severe ID and DWM [53].

VH/CH with Specific Brainstem or Cerebellar Malformation

There are several distinctive or pathognomonic radiologic appearance of the cerebellum or brainstem that should be specifically looked for when reviewing images, as they can dramatically narrow the differential diagnosis or direct management and counseling regarding prognostication. We will discuss the molar tooth sign (MTS), rhombencephalosynapsis (RES), pontine tegmental cap dysplasia, brainstem disconnection, diencephalic–mesencephalic junction dysplasia, and oculocerebrocutaneous syndrome.

Molar Tooth Sign

MTS is characterized by elongated, thickened, and horizontally orientated superior cerebellar peduncles and a deep interpeduncular fossa, associated with vermian hypoplasia or dysplasia (Fig. 4a). MTS is a pathognomonic sign of Joubert syndrome and related disorders (JSRD) (MIM 616654), characterized mainly by intellectual disability, hypotonia, ataxia, ocular motor apraxia, and neonatal breathing dysregulation [54–56]. In 20% of cases, JSRD is associated with extraneural manifestations with possible involvement of the eye (retinal dystrophy), kidney (nephronophthisis), liver (fibrosis), and limbs (polydactyly). Additional brain malformations may include polymicrogyria, cortical heterotopia, agenesis of the corpus callosum, and encephalocele/cephalocele [57]. To date, more than 30 genes have been associated with JSRD, and all encode proteins that have a key role in the primary cilium, establishing JSRD as ciliopathy [58]. Primary cilia mediate various signaling processes in several developing organs including the retina, kidney, liver, and brain [59]. MTS is thought to be due to defective cilium-dependent neuronal migration and axon guidance [60]. In addition, defects in midline fusion of the developing vermis are thought to be due to impaired Wnt signalling [61] and SHH-mediated neural tube patterning and cerebellar granule cell proliferation [62].

Rhombencephalosynapsis

RES is a rare cerebellar malformation characterized by partial or complete absence of cerebellar vermis and fusion of cerebellar hemispheres and dentate nuclei [63] (Fig. 4b). Additional neuroradiological features variably reported include midline fusion of the tectum, absence of septum pellucidum, dysplastic corpus callosum, and holoprosencephaly.

Clinical presentation and prognosis are extremely variable ranging from motor delay with cognitive impairment to normal intelligence. Neurodevelopmental outcome has been shown to correlate with the severity of RES and the presence of associated brain anomalies, including hydrocephalus with aqueductal stenosis, fused colliculi, and abnormal cerebral cortex [64].

Despite this clinical heterogeneity, up to 85% of individuals with RES typically display a characteristic figure-of-eight headshaking behavior, a stereotypic hallmark, that may help physicians to suspect RES before performing any imaging [65, 66]. Although most RES cases are non-syndromic, RES has been reported in some individuals with Gómez–López–Hernández (GLH) syndrome (MIM 601853) and VACTERL-H (vertebral defects, anal atresia, cardiac defects, tracheoesophageal fistula, renal defects, and limb defects; MIM 314390). Whereas the genetic locus of GLH is still unknown, VACTERL-H has been recently associated with X-linked mutations in *ZIC3* (MIM 314390) and *FANCB* [67], yet no individuals with RES have been reported to carry mutations in those genes so far. Interestingly, C-terminal mutations in *MN1*, a gene important for craniofacial and CNS development, have been recently linked to syndromic intellectual disability (CEBALID syndrome, MIM 618774), presenting with RES [68]. There does not seem to be any evidence of prenatal events or risk factors associated with RES [69]. Though rare, reports of intra-familial recurrence, consanguinity, and cytogenetic abnormalities support a possible genetic etiology [64]. Deficits in dorsal–ventral patterning of roof plate and midline cerebellar primordium at the junction of the mesencephalon and first rhombomere are hypothesized pathophysiological mechanisms [64, 69].

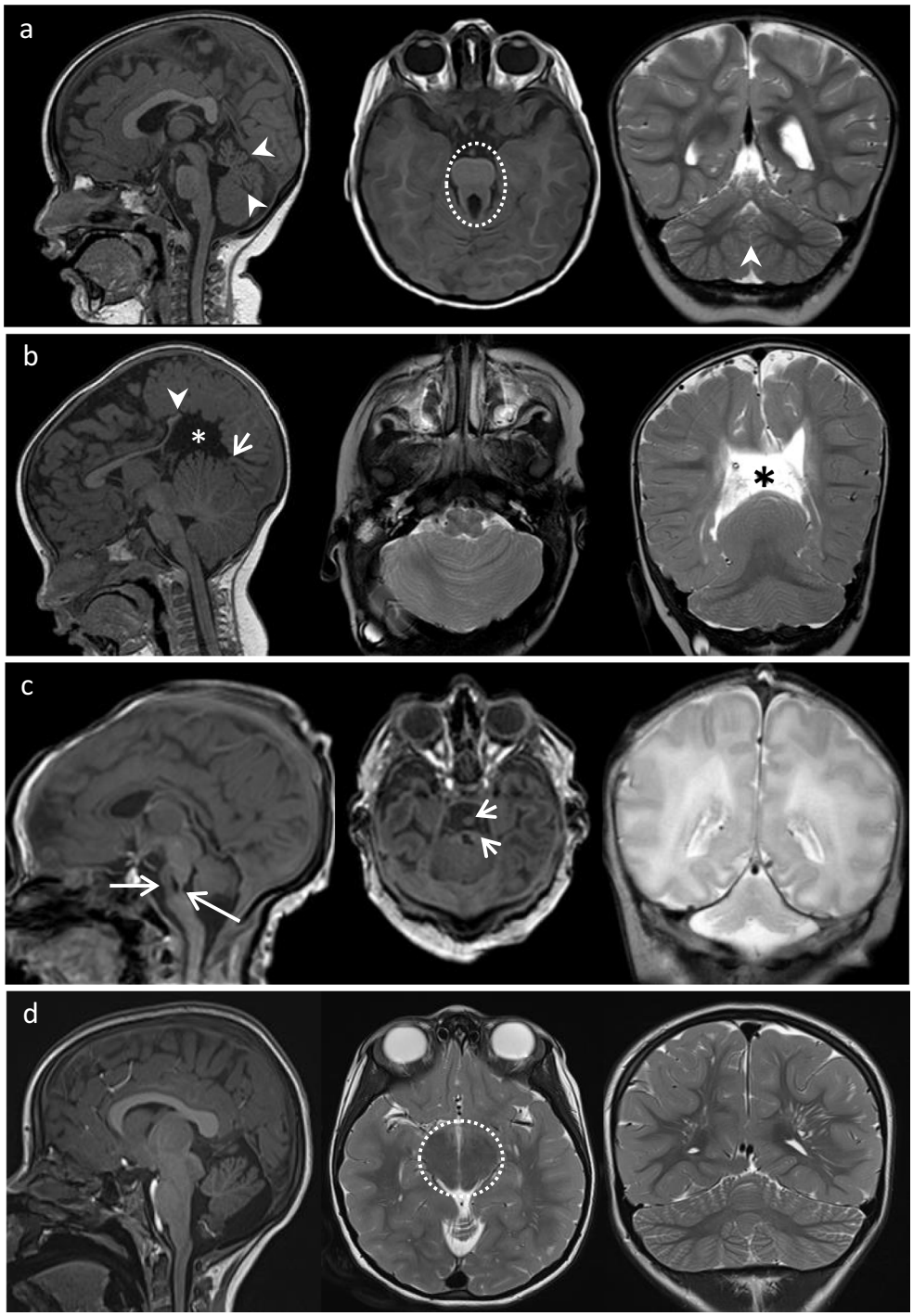

Fig. 4 Specific brainstem and cerebellar anomalies. Sagittal (left panels), axial (middle panels), and coronal (right panels) MRIs. **a** Molar tooth sign (MTS) in a patient with Joubert syndrome. The cerebellar vermis is hypoplastic (arrowhead), and the MTS (dotted circle) is appreciated on axial images, formed by the elongated, thickened, and horizontally orientated superior cerebellar peduncles. **b** Rhombencephalosynapsis. Absence of the cerebellar vermis and fusion of the cerebellar hemispheres are best appreciated on axial and coronal views. Other midline abnormalities are present including midline CSF cyst (white asterisk) causing a cranial displacement of the splenium of the corpus callosum (arrowhead), hypoplasia of the tentorium (arrow) resulting in upward herniation of the cerebellum, and agenesis of the septum pellucidum (black asterisk). **c** Brainstem disconnection. Hypoplasia of the cerebellar vermis and hemispheres associated with markedly small pons and presence of two thin bands of tissue (arrows) connecting the midbrain and the medulla. **d** Diencephalic–mesencephalic junction dysplasia. The butterfly-like appearance of the midbrain (dotted circle) is formed by the downward displacement of the diencephalic–mesencephalic junction and the anterior midbrain cleft which is contiguous with the third ventricle. The cerebellar vermis is mildly hypoplastic

Pontine Tegmental Cap Dysplasia

Pontine tegmental cap dysplasia (PTCD) (MIM 614688) is characterized by absence of the ventral pontine prominence, with a vaulted pontine tegmentum (the "cap") [70]. Severely affected patients have a "beak-like" prominence on the dorsal pons, with a kinked brainstem. Additional neuroimaging findings include hypoplastic or absent inferior cerebellar peduncles, hypoplastic middle cerebellar peduncles, VH, a MTS-like aspect of the pontomesencephalic junction, and absent inferior olivary prominence [70, 71]. Affected individuals present with multiple cranial nerve deficits including facial paralysis, trigeminal anesthesia, swallowing dysfunction, and hearing loss. Additionally, congenital heart, kidney, vertebral, and rib defects have been described [72]. Neurodevelopmental outcome can be extremely variable and seems to correlate with the degree of brainstem involvement, as patients with severe brainstem dysplasia ("beak-like")

usually die early in life, whereas others with milder neuroradiological phenotype survive and may have normal intelligence. PTCD is presumed to be an axonal guidance disorder [71], although the genetic cause remains unknown and no familial recurrence has been reported [73].

Brainstem Disconnection

Brainstem disconnection (BD) is a rare posterior fossa abnormality characterized by total or subtotal absence of a brainstem segment, with the rostral and caudal brainstem portions connected only by a thin cord of tissue (Fig. 4c). Among the 14 patients reported so far, only one survived after infancy, whereas others had very poor outcome, dying within the first 2 months of life [74]. BD has been classified as pontomesencephalic, pontomedullary, or pontocervical according to the region of the brainstem that is most affected. Cerebellar hypoplasia is a constant associated finding. Extra-CNS anomalies have been variably reported, with vertebral segmentation defects and hydronephrosis most commonly observed. No intra-familial recurrence or consanguinity has been recorded so far. Although deregulated expression of *EZH2*, a histone methyltransferase, has been revealed in a recent autopsy study [75], the exact pathomechanism of BD remains unknown [60, 74].

Diencephalic–Mesencephalic Junction Dysplasia

Diencephalic–mesencephalic junction dysplasia (DMJD) refers to a poorly defined junction between the diencephalon and mesencephalon, originally described in a few patients with PCH [8]. Later, a peculiar shape of the DMJ with "butterfly"-like appearance of the midbrain on axial images was described in six cases and was claimed as a distinctive feature of this disorder [76] (Fig. 4d). The "butterfly"-like appearance of the midbrain is formed by an anterior midbrain cleft which is contiguous with the third ventricle and the downward displacement of the diencephalic–mesencephalic junction. Recently, the phenotypic spectrum of DMJ has been revisited [77], revealing that the butterfly-like appearance may be subtle and not present in all individuals with DMJD. The cerebellum is often affected with variable severity, ranging from VH to PCH. Further CNS malformations may include corpus callosum anomalies and hydrocephalus [63, 77]. Clinical findings include spastic tetraparesis, dystonia, hypothalamic dysfunction, epilepsy, and severe developmental delay.

Guemez-Gamboa et al. [78] reported that bi-allelic mutations in *PCDH12*, previously linked to a primary microcephalic disorder with brain calcification (MIM 251280), cause DMJD in a homogenous group of patients, including two of the original families previously described [76]. Most of the affected patients presented with progressive microcephaly, craniofacial dysmorphism, early onset epilepsy, severe ID, and spasticity. In addition to DMJD, brain MRI revealed thin corpus callosum, punctate brain calcifications, ventriculomegaly, and white matter tract defects. Of note, midbrain–hypothalamic dysplasia was recognized even in the first cohort without mention of "butterfly"-like appearance [79]. PCDH12 is a vascular endothelial protocadherin that promotes cellular adhesion, which is widely expressed not only in the endothelial tissues as originally thought [80] but also in the CNS, playing a crucial role in neurite outgrowth [78]. The "butterfly"-like appearance of the midbrain may reflect a disruption in cortical projections due to abnormal axonal tract formation.

Oculocerebrocutaneous Syndrome

Oculocerebrocutaneous syndrome (OCCS) (MIM 164180), also known as Dellman syndrome, is a rare neurodevelopmental disorder characterized by a triad of eye and skin anomalies [81]. Brain MRI of affected individuals shows a specific mid-hindbrain malformation, consisting of a giant dysplastic tectum, and absent or severely malformed vermis. Additional brain malformations include frontal predominant polymicrogyria and periventricular nodular heterotopia, agenesis of the corpus callosum, enlarged lateral ventricles, or hydrocephalus. Clinically, affected individuals present with orbital cysts, anophthalmia/microphthalmia, focal aplastic or hypoplastic skin defects, and skin appendages. OCCS is thought to be genetic but the exact etiology remains unknown [82].

VH/CH and Brainstem Hypoplasia

The brainstem includes the midbrain, the pons, and the medulla oblongata. Traditionally, a normal pons has a rostrocaudal length twice that of the midbrain (from the isthmus to the third ventricle), whereas the rostrocaudal length of the midbrain should be approximately the same of the medulla (from the level of the obex to the level of the ventral pontomedullary junction) (Fig. 2A) [27]. The employment of the recently identified reference biometric data of brainstem [23] will provide further insights into the normal brainstem morphology and its components.

Pontocerebellar Hypoplasia

PCH encompasses a heterogenous group of inherited autosomal recessive neurodegenerative disorders with prenatal onset of cerebellar and pons hypoplasia and atrophy (Fig. 5b). Microcephaly and motor and cognitive impairments are present in almost all individuals, whereas cortical atrophy, thin corpus callosum, seizure, and optic atrophy are variably reported.

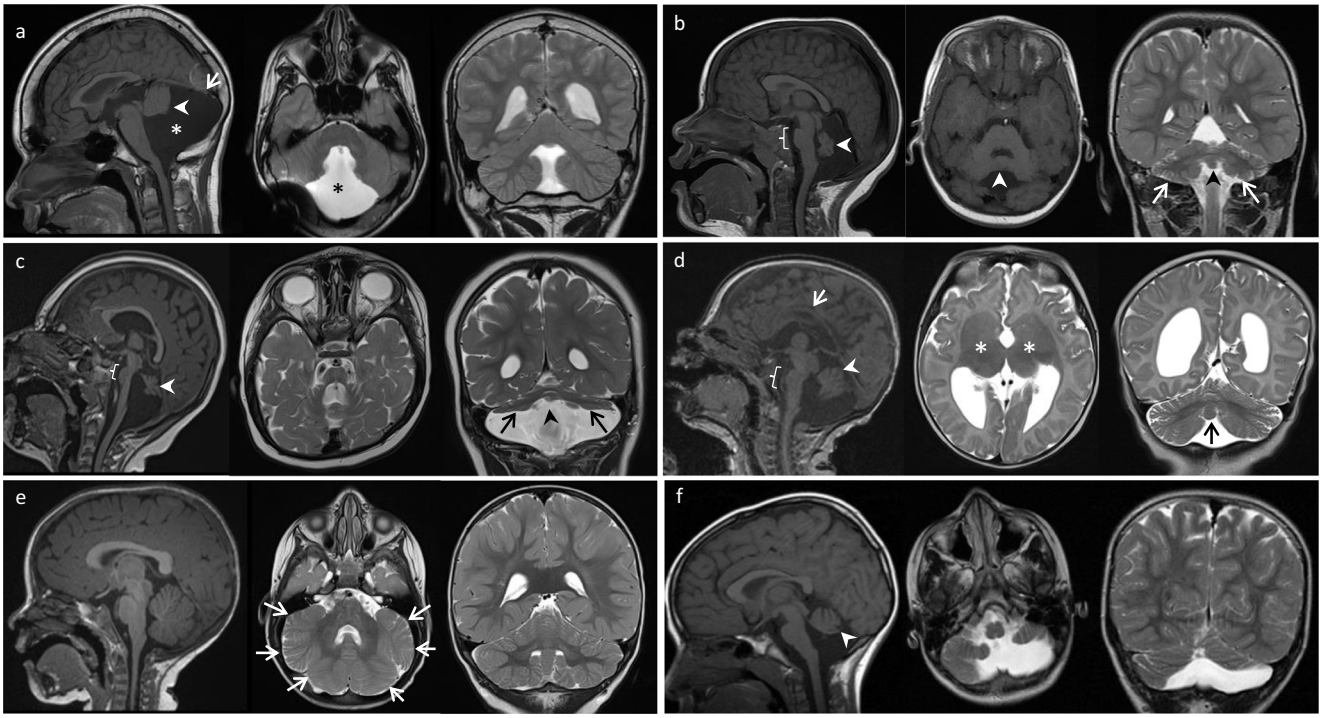

Fig. 5 Examples of cerebellar hypoplasia with or without pontine hypoplasia and cortical anomalies. **a** Dandy–Walker malformation. Note the enlarged posterior fossa, hypoplastic and upwardly rotated vermis (arrowhead), dilatation of the fourth ventricle resulting in a cystic appearance of the posterior fossa (asterisk), and elevation of the tentorium (arrow). **b** Pontocerebellar hypoplasia. Severe hypoplasia of the cerebellar vermis (arrowhead) and hemispheres, with reduced size and rostrocaudal length of pons. **c** CASK-related pontocerebellar hypoplasia. Note severe hypoplasia of pons and cerebellar vermis (arrowhead) and hemispheres (arrows). **d** Tubulinopathy-associated cerebellar hypoplasia and cerebral anomalies. This patient with a *TUBB* mutation has typical radiologic findings associated with tubulinopathies which include hypoplasia of the cerebellar vermis (arrowhead) and pons, hypoplasia of the corpus callosum (arrow), and dysmorphic and fused basal ganglia (asterisks). **e** Cerebellar dysplasia. Note the normal size but abnormal foliation and orientation of the cerebellar cortex in both hemispheres. The vermis and brainstem are normal. **f** Asymmetric cerebellar hypoplasia. Inferior vermis hypoplasia (arrowhead) and left > right cerebellar hemisphere hypoplasia

To date, there are 11 formally recognized PCH types with 17 causal genes identified (for recent review, see Van Dijik et al. [83]). Most PCH genes play a role in RNA processing and protein translation [84]: *TSEN54*, *TSEN2*, *TSEN34*, *CLP1*, and *TOE1* encode subunits of the tRNA splicing endonuclease complex, whereas *EXOSC3* and *EXOSC8* encode exosome complexes, *RARS2* a mitochondrial tRNA arginyl synthetase, and *AMPD2* adenosine monophosphate deaminase 2 (Table 1).

Despite significant overlaps, specific neuroradiological hallmarks have been traditionally recognized among various PCHs, such as a "dragonfly appearance" of the cerebellum in PCH2 and PCH4 [85] and a "figure-of-8" appearance of the brainstem in PCH9 [86, 87]. PCH1 (MIM 607596 and MIM 614678) is linked to mutations in *VRK1* [88], *EXOSC3* [89], *EXOSC8* [90], and *SLC25A46* [91], and is characterized by spinal muscular atrophy, resulting in substantial global weakness, decreased or absent reflexes, dysphagia, and respiratory distress. Hypoplasia and atrophy of the pons and cerebellum may be moderate on neuroimaging in PCH1. Some *EXOSC3* cases with mostly a spinal muscular atrophy (SMA)-like presentation have been reported to have normal cerebellar and pons appearance during first months of life [92]. PCH2 (MIM 277470, MIM 612389, MIM 612390, MIM 613811, MIM 617026) is the most prevalent of all PCH subtypes and is characterized by generalized myoclonus, dysphagia, dystonia, chorea, and progressive microcephaly. The PCH observed on imaging is severe. PCH2 is associated with mutations in tRNA splicing endonucleases genes (*TSEN54*, *TSEN34*, *TSEN2*, *TSEN15*) as well as a selenium transferase (*SEPSEC5*) and a subunit of the Golgi-associated retrograde protein (*VPS53*) [93–95]. *TSEN54* is the most common cause of all PCHs [96–99]. PCH3 (MIM 608027), described in only one family so far, is associated with thin corpus callosum and optic atrophy on brain MRI, and is linked to a homozygous mutation in the *PCLO* gene [100].

Individuals with PCH4 (MIM 225753) and PCH5 (MIM 610204) have the most severe clinical phenotype, with congenital contractures and polyhydramnios and a lethal course in the neonatal period [83, 85]. Interestingly, *TSEN54* mutations account for a phenotypic spectrum from the mildest clinical presentation in PCH type 2 to the most severe phenotype in PCH4 and PCH5 [85]. The presence of elevated CSF lactate may help to recognize PCH6 (MIM 611523), an early-

infantile epileptic encephalopathy presenting with PCH and caused by bi-allelic mutations in the mitochondrial arginyl-tRNA synthetase gene, *RARS2* [101]. PCH7, typically characterized by ambiguous genitalia, has been recently linked to bi-allelic mutations in *TOE1*, which is involved in pre-mRNA splicing [102]. Loss-of-function mutations in *CHMP1A* [103] have been associated with PCH8 (MIM 614961), typically showing postanal microcephaly, PCH with proportionate vermis and hemisphere hypoplasia and congenital contractures. In addition to the "figure-of-8" appearance of brainstem and PCH, individuals with PCH9 usually show hypodysgenesis of corpus callosum, ventriculomegaly, poor neurodevelopmental outcome, and possible neuropathy [86, 104]. A recurrent missense homozygous mutation in *CLP1*, a RNA kinase involved in tRNA splicing and maturation, has been reported in some individuals with PCH and possible peripheral nervous system involvement, namely PCH10 [105]. Recently, a non-degenerative form of PCH (PCH11) (MIM 617696) has been linked to loss-of-function mutations in *TBC1D23*, a gene mainly involved in vesicular trafficking, cortical development, and immunity [106, 107]. Lastly, bi-allelic variants in *MINPP1*, a gene involved in the hydrolysis of inositol phosphate in the endoplasmatic reticulum [108], have been reported in several subjects displaying PCH and other brain anomalies, microcephaly, and additional features such as epilepsy, micropenis, and cataracts [108, 109]. An incessant growing literature of novel disorders presenting with PCH will expand soon the number of PCH subtypes [83, 110, 111].

CASK-Related PCH

Heterozygous loss-of-function mutations in the X-linked *CASK* gene are associated with progressive microcephaly, hypoplasia of the pons and cerebellum (with usually similar involvement of cerebellar hemispheres and vermis, Fig. 5c), ID, and epilepsy in females [112–115]. In contrast to the previously discussed PCHs, CASK-related PCH is not a progressive neurodegenerative disorder. The severity of the pontocerebellar hypoplasia observed on MRI is not of prognostic value [113]. Supratentorial structures are usually spared, although reduction of frontal gyri and cortical atrophy may occur [112, 116]. The phenotype in males ranges from severe epileptic encephalopathy with progressive microcephaly and PCH to a milder phenotype due to mosaicism or hypomorphic mutations [115, 116].

Congenital Disorders of Glycosylation

Congenital disorders of glycosylation (CDG) are a group of inborn errors of metabolism caused by defects in several synthetic pathways of glycans, including N- and O-linked defects. *PMM2*-CDG (CDG1a) is by far the most frequent among the N-linked glycosylation defects, displaying a multisystemic involvement [117]. Accordingly, the clinical picture may be very broad, including eye anomalies, coagulation defects, neuropathy, impaired liver function, and abnormal fat distribution. Similarly, the neurodevelopmental outcome is extremely variable.

The cerebellum is typically affected in individuals carrying bi-allelic mutations in *PMM2* gene with a phenotypic spectrum ranging from isolated cerebellar hypoplasia (affecting mainly the anterior vermian lobe) to more commonly progressive cerebellar and pons atrophy, mimicking PCH cases. Additional neuroradiological features may include olivopontocerebellar hypotrophy/hypoplasia, Dandy–Walker appearance, and cerebellar cortical hyperintensity [118, 119]. Cerebellar involvement has also been observed in individuals with *SRD5A3*-CDG [120, 121] and occasionally in other CDGs [122]. Although the role of N-glycosylation protein in cerebellar/hindbrain development is largely unknown, it has been suggested that the observed malformations may be the result of abnormal protein folding and response to endoplasmic reticulum (ER) stress [123].

Of note, though serum transferrin isoelectrofocusing is widely used as a screening for N-glycosylation disorders, a normal serum transferrin pattern does not exclude CDG due to possible false-negative results [124]. Therefore, a CDG gene panel should be ordered if CDG is highly suspected based on clinical and neuroradiological findings despite normal serum transferrin patterns.

Cerebellofaciodental Syndrome: *BRF1*-Related PCH

Bi-allelic mutations in *BRF1* gene, which encodes an RNA polymerase III transcription initiation factor subunit, have been associated with cerebellofaciodental syndrome (MIM 616202), an autosomal recessive disorder characterized by microcephaly, short stature, ID, cerebellar and brainstem hypoplasia, and dysmorphic features including taurodontism. Similar to some hypomyelinating leukodystrophies caused by mutations in genes encoding Pol III subunits or tRNA processing factors [125, 126], *BRF1* mutations reduce Pol III–related transcription activity and result in abnormal hindbrain development [127, 128].

Osteogenesis Imperfecta, Type XV or WNT1-Related PCH

A variable degree of cerebellar and brainstem hypoplasia has been reported in autosomal recessive osteogenesis imperfecta (MIM 615220) due to mutations in *WNT1* [58]. *WNT1* is expressed in the developing rhombic lip and hindbrain precerebellar nuclei [129, 130] where it plays a pivotal role in signaling cascades that generate midbrain dopamine and cerebellum neurons. Of note, the Wnt1 mouse model displays

developmental defects of the midbrain, pons, and cerebellum, similar to the human WNT1 phenotype [131, 132].

VH/CH with Brainstem and Cortical Migration Anomalies

Tubulinopathies

Tubulinopathies are a wide and overlapping range of brain malformations caused by mutations in one of seven genes encoding different tubulin isotypes, namely alpha-tubulin (*TUBA1A*), beta-tubulin (*TUBB2A*, *TUBB2B*, *TUBB3*, *TUBB4A*, *TUBB*), and gamma-tubulin (*TUBG1*) isoforms [133]. Tubulin proteins form heterodimers that incorporate into microtubules. Microtubules are polarized cytoskeletal structures essential for mitosis and intracellular trafficking that play a crucial role in neurogenesis, neuronal migration, and post-migrational organization [134]. The principal cerebellar anomalies associated with tubulinopathies are cortical dysplasia and hypoplasia [135–137], and these are consistently part of more complex neuroradiological cerebral anomalies that may include lissencephaly, polymicrogyria, microlissencephaly and simplified gyration, enlarged tectum, pons hypoplasia, thin/absent corpus callosum, and dysmorphic basal ganglia. Fusion of the caudate nucleus and putamen with absence of the anterior limb of the internal capsule is very evocative of tubulinopathies (Fig. 5d) [133, 137, 138]. Some genotype–phenotype correlations can be made. *TUBA1A* mutations are associated with lissencephaly/microlissencephaly and *TUBB2B* mutations with polymicrogyria-like cortical dysplasia [133]. The constellation of mild to severe CH and dysplasia (with predominant vermis involvement) in association with brainstem hypoplasia, hypodysgenesis of corpus callosum, and dysmorphic basal ganglia represents the distinctive brain MRI pattern of tubulinopathies and is present in up to 78% of individuals, mostly carrying heterozygous mutations in *TUBA1A*, *TUBB2B*, or *TUBB3* [133].

Tubulin-Like Phenotype Due to *DDX3X* Mutations

Recently, a tubulin-like phenotype has been described in a subset of females harboring pathogenic variants in *DDX3X* [29, 139], a known X-linked ID gene (MIM 300958). *DDX3X* encodes an ATP-dependent "DEAD-box" RNA helicase involved in RNA processing and has been shown to exert a pivotal role in neurite outgrowth and dendritic spine formation through the translational activation of mRNAs involved in Rac1 activation [140]. Main neuroradiological features include bilateral frontal and perisylvian polymicrogyria and/or dysgyria, callosal hypodysgenesis, dysmorphic basal ganglia with indistinct anterior limbs of internal capsules, incomplete hippocampal rotation, and pontine and inferior vermis hypoplasia. DDX3X is thought to act through a similar pathogenic mechanism as tubulinopathies, involving altered microtubule stability and defective migration of cortical GABAergic interneurons due to impaired Rac1 signaling [141].

RELN/VLDLR-Related CH

The association of PCH with lissencephaly spectrum on neuroimaging is also typically reported in individuals with a defect in the reelin pathway, a critical signaling pathway that regulates radial neuronal migration and cell layer formation in both the cerebral cortex [142, 143] and cerebellum [143]. Bi-allelic mutations in *RELN* and its receptor *VLDLR* have been reported in patients with cerebellar, pontine, and cerebral cortical anomalies. Although VH with poor foliation is observed in both conditions, hemispheric involvement is less pronounced in VLDLR-mutated patients with some folia still identifiable [144]. Similarly, lissencephaly/pachygyria is more pronounced in individuals with *RELN* mutations, whereas mild simplification or thickening of cortical gyration is part of the VLDLR spectrum [144].

Cobblestone Cerebral Cortex Disorders: Dystroglycanopathies and GPR56/COL3A1-Related Cobblestone Cortex

The muscular dystrophy–dystroglycanopathies (MDDG) are a heterogeneous group of congenital muscular dystrophies (CMD) characterized by a defective O-mannosylation of α-dystroglycan due to mutations in an increasing number of genes (Table 1) [117]. MDDG are systematically divided in several categories based on their different clinical presentation. CH has been typically described in the most severe end of the phenotypic spectrum of MDDG, including CMD with cerebellar involvement (e.g., Fukuyama muscular dystrophy), muscle–eye–brain disease, and Walker–Warburg syndrome. Walker–Warburg syndrome represents the most severe phenotype, presenting with small and dysmorphic cerebellar hemispheres (often with cysts), absent vermis and brainstem hypoplasia, abnormal tectum and corpus callosum, ventriculomegaly, and cortical anomalies including cobblestone cerebral cortex, lissencephaly, pachygyria, and polymicrogyria [145, 146]. Cobblestone malformations are a recognizable neuronal migration disorder characterized by protrusions of neurons beyond the first cortical layer at the pial surface of the brain [147]. Microcephaly, eye abnormalities (e.g., cataracts, congenital glaucoma, microphthalmia), neonatal hypotonia, and increased serum creatine kinase (CK) are additional findings that may help in suspecting a MDDG diagnosis. Of note, it is important for the clinician to be careful not to overlook possible muscular involvement even in the presence of the dramatic central nervous system malformations.

A cobblestone-like appearance of the cortex in combination with CH has also been observed in GPR56-related polymicrogyria (MIM 606854), a neurodevelopmental disorder caused by bi-allelic mutations in *ADGRG1* (also known as *GPR56*). Affected patients usually present with bilateral frontoparietal cobblestone-like "polymicrogyria," cerebellar hypoplasia/dysplasia with cysts mainly affecting the superior vermis, myelination abnormalities, and variable corpus callosum anomalies. In contrast to the cobblestone malformations described in MDDG, the brainstem is less severely affected [148]. Lastly, bi-allelic mutations in *COL3A1*, a collagen gene responsible for autosomal dominant Ehlers–Danlos syndrome type IV (MIM 130050), have been linked to a similar neuroradiological phenotype [149, 150]. In addition to Ehlers–Danlos features, brain MRI of affected patients show cerebellar hypoplasia (mainly of the vermis) and/or dysplasia with cysts, pons hypoplasia, cobblestone cortex, and diffuse hypomyelination. Interestingly, *COL3A1* encodes the proα1(III) chains of type III procollagen, a ligand of ADGRG1 (GPR56). Interaction of GPR56 with COL3A1 regulates cortical development and lamination by inhibiting neuronal migration through activation of the RhoA pathway [151, 152].

Rare Disorders Due to *CDK5*, *PI4KA*, *WDR81*, *KIAA1109*, *MACF1*, *MAST1*, and *CTNNA2* Mutations

Novel neurodevelopmental disorders showing involvement of cerebellum, brainstem, and cortex are continuously being reported.

A severe phenotype characterized by cerebellar hypoplasia, small pons, lissencephaly, agenesis of corpus callosum, and microcephaly has been linked to a loss-of-function homozygous mutation in *CDK5* in a consanguineous Israeli Moslem family [153]. Interestingly, CDK5 is a cyclin-dependent kinase that has been shown to have a crucial role in Purkinje cell dendritic growth [154] and cerebral cortical folding of upper-layer neurons [155].

Compound heterozygous variants in *PI4KA* have been identified in three fetuses of the same family showing perisylvian polymicrogyria, VH, dysplastic dentate nuclei, pons hypoplasia (in one case), and arthrogryposis [156]. Of note, *PI4KA* encodes a phosphatidylinositol 4-kinase which is involved in the biosynthesis of phosphatidylinositol 4,5-bisphosphate, an important substrate of phosphoinositide and PI3K-AKT-mTOR signaling pathways.

A wide phenotype, including microcephaly, PCH, and lissencephaly at its most severe spectrum, has been associated with bi-allelic mutations in *WDR81*, a gene with a crucial role in mitotic progression and Purkinje cell survival [157–159].

Recently, bi-allelic loss-of-function/hypomorphic mutations in *KIAA1109* have been identified in several individuals with CH, brainstem dysgenesis, lissencephaly/pachygyria, possible ventriculomegaly, clubfoot/arthrogryposis, cardiac and ophthalmologic anomalies [160].

Heterozygous missense variants and an in-frame deletion involving highly conserved zinc-binding residues within the microtubule-binding GAR domain of *MACF1* (microtubule actin crosslinking factor 1) have been recently linked to a complex brain malformation characterized by predominantly posterior pachygyria/lissencephaly, hypoplastic and dysplastic brainstem, variably short corpus callosum, and mild to moderate VH/CH hypoplasia, the latter being less pronounced than the brainstem anomalies [161]. On axial images, the medulla has a striking "W" shape formed by its very wide and flat shape and small pyramids.

Heterozygous mutations in *MAST1*, another gene encoding a microtubule-associated protein, cause a neurodevelopmental disorder characterized by an enlarged corpus callosum, CH (vermis > hemisphere hypoplasia), brainstem (mainly the pons) hypoplasia, ventricular dilatation, and cortical malformations ranging from subtle dysgyria to a tubulin-like phenotype [162].

Lastly, bi-allelic truncating mutations have been reported in *CTNNA2* in 7 subjects with a distinct recessive form of pachygyria associated with hypodysgenesis of the corpus callosum, CH, and possible brainstem hypoplasia.

VH/CH with Cerebellar Dysplasia

Cerebellar dysplasia is characterized by abnormalities of cerebellar foliation, fissuration, white matter arborization, and gray–white matter junction on brain MRI (Fig. 5e) [27]. It is often associated with a range of complex neurodevelopmental disorders such as JSRD, tubulinopathies, alphadystroglycanopathies and GPR56/*COL3A1*-related polymicrogyria. When the cerebellar dysplasia is focal and unilateral in a cerebellar hemisphere of reduced volume, a prenatal acquired etiology is assumed, especially in the presence of hemorrhages on MRI. A diagnostic workflow for cerebellar dysplasia and related disorders is illustrated in Fig. 6.

Poretti–Boltshauser syndrome (PBS; MIM 150320), caused by bi-allelic *LAMA1* mutations [163], and cobblestone cerebral cortex disorders [164] are characterized by the presence of CH/CD and cerebellar cysts. The cerebellar dysplasia in these disorders is thought to arise from basement membrane defects resulting in abnormal neuronal migration. Chudley–McCullough syndrome (MIM 604213) is a highly recognizable clinico-radiological entity characterized by sensorineural deafness, agenesis of the corpus callosum, frontal polymicrogyria, quadrigeminal plate cyst, and ventricular enlargement in addition to dysplasia of the inferior cerebellar hemispheres with possible VH. Chudley–McCullough syndrome is caused by bi-allelic mutations in *GPSM2*, which encodes a GTPase regulator needed for correct mitotic spindle

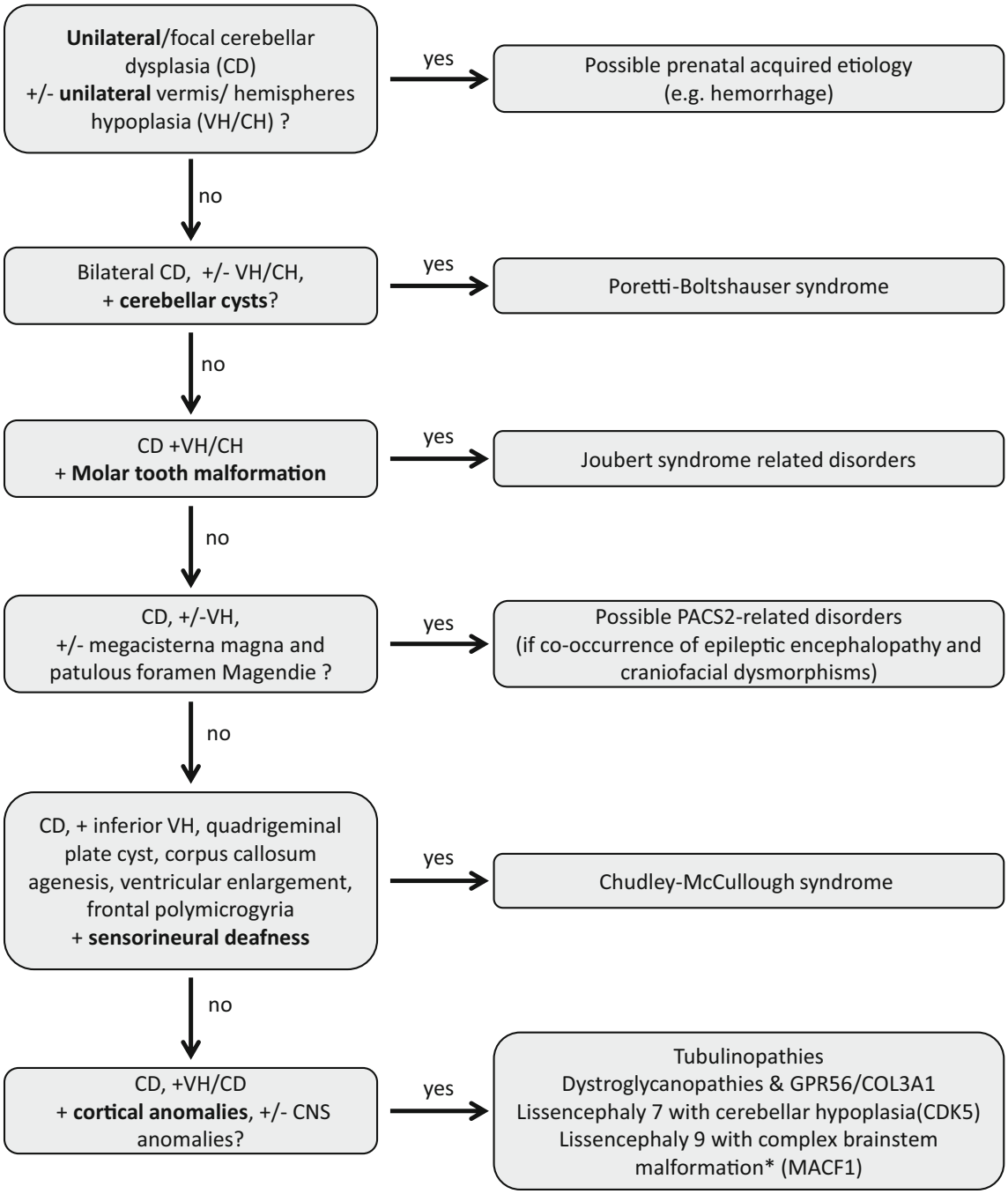

Fig. 6 Diagnostic algorithm of cerebellar dysplasia and related anomalies. CD, cerebellar dysplasia; CH, cerebellar hypoplasia; DWM, Dandy–Walker malformation; PCH, pontocerebellar hypoplasia; VH, vermis hypoplasia

orientation during stem cell division [165]. Recently, a crucial role of Gpsm2 in the regulation of actin dynamics in epithelial and neuronal tissues has been elucidated [166]. Cerebellar dysgenesis (along with VH, mega cisterna magna and patulous foramen Magendie) can also be part of the PACS2-related epileptic encephalopathy, a recently identified mendelian disorder whose main features are epilepsy, ID, and craniofacial dysmorphisms. *PACS2* is a trans-Golgi membrane traffic regulator gene highly expressed during human embryonic brain development, but its role in cerebellum is yet unknown [167].

Practical Approach to the Diagnosis of Cerebellar Hypoplasia

Accurate diagnosis of patients with cerebellar hypoplasia requires a multidisciplinary team approach. First, a careful

review of medical history and a physical examination, involving the pediatrician, neurologist, and clinical geneticist, are the first steps to generate a thorough phenotypic characterization. Concurrently, the brain MRI should be reviewed with a neuroradiologist to seek any possible hallmark of acquired causes (e.g., hemorrhage in preterm infants, hemosiderin on susceptibility-weighted imaging, cerebellar clefts) and should be compared with previous imaging if available to assess for possible signs of progression and cerebellar atrophy. Once acquired etiologies are ruled out, we suggest relying on our proposed algorithm (Fig. 3) to determine which of the six CH classes the malformation corresponds to.

Thereafter, the diagnostic work-up should be customized for each cerebellar subgroup. Array-CGH should be performed in all VH/CH and DWM cases. If the clinical assessment points to a specific syndrome (e.g., CHARGE), targeted genetic testing should be organized. In the absence of clinical clues, a broad ID panel (preferably trio-based which includes proband and parents), or WES\WGS if available, should be offered to all VH/CH cases with associated ID. Despite possible false-negatives, isoelectric focusing of serum transferrin should be performed if a congenital disorder of glycosylation is suspected based on clinical and neuroradiological findings. Determination of CK level should be considered as increased levels may provide clue to an α-dystroglycanopathy. Specific panels including genes related to the corresponding cerebellar subgroups (for example a JSRD gene panel for patients with a MTS, a PCH gene panel in patients with PCH) should be pursued. If available, WES may be performed as a first step, first looking through a bioinformatic customized panel of genes known to be associated with the identified cerebellar class, and if this yields negative results, the analysis should be expanded to include a broader set of genes not yet associated with that phenotype and potential new candidate genes.

Conclusions

Cerebellar hypoplasias are an extremely heterogenous group of disorders with a wide range of etiologies, radiologic characteristics, clinical features, and neurodevelopmental outcomes. Recent advances in genetic methods such a whole-exome and -genome sequencing have allowed the continuous identification of novel CH-related disorders, providing insight into the complexity of cerebellar development. Nevertheless, the exact genetic or acquired etiologies remain unknown in a considerable number of disorders, such as isolated VH and CH, RES, and PCH. Accurate classification of cerebellar malformations is key for diagnosis, work-up, and prognosis; however, we still do not have a standard recognized classification system that integrates neuroimaging and molecular genetic and developmental biological criteria.

A neuroimaging-based classification remains a useful initial practical approach to classify CHs into one of six subcategories, based on whether the CH is isolated or associated with posterior CSF anomalies, specific midbrain or cerebellar malformations, brainstem hypoplasia with or without cortical migration anomalies, or dysplasia. Combining imaging, neurological and dysmorphological assessments enable prompt recognition and diagnosis of a specific CH, which will allow the clinician to (1) perform appropriate genetic testing and recurrence risk counseling, (2) screen for associated comorbidities, and (3) offer more precise neurodevelopmental prognosis. All these efforts will lead to a better understanding of molecular and clinical aspects of CH that may be pivotal to develop novel therapeutic strategies in the future.

Acknowledgments We would like to thank Emma Hoang with her assistance in drawing the figures.

Funding MS hold a Junior 2 Chercheurs-Boursiers Cliniciens salary award from the Fonds de recherche du Québec – Santé.

Compliance with Ethical Standards

Conflict of Interest The authors declare that they have no conflict of interest.

References

1. von Bartheld CS, Bahney J, Herculano-Houzel S. The search for true numbers of neurons and glial cells in the human brain: a review of 150 years of cell counting. J Comp Neurol. 2016;524:3865–95.
2. Stoodley CJ, Limperopoulos C. Structure-function relationships in the developing cerebellum: evidence from early-life cerebellar injury and neurodevelopmental disorders. Semin Fetal Neonat Med. 2016;21:356–64.
3. Guell X, Gabrieli JDE, Schmahmann JD. Triple representation of language, working memory, social and emotion processing in the cerebellum: convergent evidence from task and seed-based resting-state fMRI analyses in a single large cohort. NeuroImage. 2018;172:437–49.
4. Ramos TC, Balardin JB, Sato JR, Fujita A. Abnormal cortico-cerebellar functional connectivity in autism spectrum disorder. Front Syst Neurosci. 2018;12:74.
5. Marien P, Ackermann H, Adamaszek M, Barwood CH, Beaton A, Desmond J, et al. Consensus paper: language and the cerebellum: an ongoing enigma. Cerebellum (London, England). 2014;13:386–410.
6. Wyciszkiewicz A, Pawlak MA, Krawiec K. Cerebellar volume in children with attention-deficit hyperactivity disorder (ADHD). J Child Neurol. 2017;32:215–21.
7. Poretti A, Boltshauser E, Doherty D. Cerebellar hypoplasia: differential diagnosis and diagnostic approach. Am J Med Genet C: Semin Med Genet. 2014;166c:211–26.
8. Barkovich AJ, Millen KJ, Dobyns WB. A developmental classification of malformations of the brainstem. Ann Neurol. 2007;62:625–39.

9. Poretti A, Boltshauser E, Huisman TA. Congenital brain abnormalities: an update on malformations of cortical development and infratentorial malformations. Semin Neurol. 2014;34:239–48.
10. Poretti A, Boltshauser E, Huisman TA. Pre- and postnatal neuroimaging of congenital cerebellar abnormalities. Cerebellum (London, England). 2016;15:5–9.
11. Poretti A, Boltshauser E, Huisman TA. Prenatal cerebellar disruptions: neuroimaging spectrum of findings in correlation with likely mechanisms and etiologies of injury. Neuroimaging Clin N Am. 2016;26:359–72.
12. Abdel Razek AA, Castillo M. Magnetic resonance imaging of malformations of midbrain-hindbrain. J Comput Assist Tomogr. 2016;40:14–25.
13. Butts T, Green MJ, Wingate RJ. Development of the cerebellum: simple steps to make a 'little brain'. Development (Cambridge, England). 2014;141:4031–41.
14. Benagiano V, Rizzi A, Lorusso L, Flace P, Saccia M, Cagiano R, et al. The functional anatomy of the cerebrocerebellar circuit: a review and new concepts. J Comp Neurol. 2018;526:769–89.
15. Marzban H, Del Bigio MR, Alizadeh J, Ghavami S, Zachariah RM, Rastegar M. Cellular commitment in the developing cerebellum. Front Cell Neurosci. 2014;8:450.
16. Beckinghausen J, Sillitoe RV. Insights into cerebellar development and connectivity. Neurosci Lett. 2019;688:2–13.
17. Yamada M, Seto Y, Taya S, Owa T, Inoue YU, Inoue T, et al. Specification of spatial identities of cerebellar neuron progenitors by ptf1a and atoh1 for proper production of GABAergic and glutamatergic neurons. J Neurosci. 2014;34:4786–800.
18. Yeung J, Ha TJ, Swanson DJ, Goldowitz D. A novel and multivalent role of Pax6 in cerebellar development. J Neurosci. 2016;36:9057–69.
19. De Luca A, Cerrato V, Fuca E, Parmigiani E, Buffo A, Leto K. Sonic hedgehog patterning during cerebellar development. Cell Mol Life Sci. 2016;73:291–303.
20. Wang L, Liu Y. Signaling pathways in cerebellar granule cells development. Am J Stem Cells. 2019;8:1–6.
21. Ten Donkelaar HJ, Lammens M. Development of the human cerebellum and its disorders. Clin Perinatol. 2009;36:513–30.
22. Lerman-Sagie T, Prayer D, Stocklein S, Malinger G. Fetal cerebellar disorders. Handb Clin Neurol. 2018;155:3–23.
23. Jandeaux C, Kuchcinski G, Ternynck C, Riquet A, Leclerc X, Pruvo JP, et al. Biometry of the cerebellar vermis and brain stem in children: MR imaging reference data from measurements in 718 children. AJNR Am J Neuroradiol. 2019;40:1835–41.
24. Boltshauser E. Cerebellum-small brain but large confusion: a review of selected cerebellar malformations and disruptions. Am J Med Genet A. 2004;126a:376–85.
25. Poretti A, Boltshauser E. Terminology in morphological anomalies of the cerebellum does matter. Cerebellum Ataxias. 2015;2:8.
26. Poretti A, Wolf NI, Boltshauser E. Differential diagnosis of cerebellar atrophy in childhood: an update. Neuropediatrics. 2015;46:359–70.
27. Poretti A, Boltshauser E, Huisman TA. Cerebellar and brainstem malformations. Neuroimaging Clin N Am. 2016;26:341–57.
28. Bosemani T, Poretti A. Cerebellar disruptions and neurodevelopmental disabilities. Semin Fetal Neonatal Med. 2016;21:339–48.
29. Aldinger KA, Timms AE, Thomson Z, Mirzaa GM, Bennett JT, Rosenberg AB, et al. Redefining the etiologic landscape of cerebellar malformations. Am J Hum Genet. 2019;105:606–15.
30. Gano D, Barkovich AJ. Cerebellar hypoplasia of prematurity: causes and consequences. Handb Clin Neurol. 2019;162:201–16.
31. Garzon MC, Epstein LG, Heyer GL, Frommelt PC, Orbach DB, Baylis AL, et al. PHACE syndrome: consensus-derived diagnosis and care recommendations. J Pediatr. 2016;178(24–33):e22.
32. Massoud M, Cagneaux M, Garel C, Varene N, Moutard ML, Billette T, et al. Prenatal unilateral cerebellar hypoplasia in a series of 26 cases: significance and implications for prenatal diagnosis. Ultrasound Obstet Gynecol. 2014;44:447–54.
33. Leibovitz Z, Guibaud L, Garel C, Massoud M, Karl K, Malinger G, et al. The cerebellar "tilted telephone receiver sign" enables prenatal diagnosis of PHACES syndrome. Eur J Paediatr Neurol. 2018;22:900–9.
34. Bolduc ME, Limperopoulos C. Neurodevelopmental outcomes in children with cerebellar malformations: a systematic review. Dev Med Child Neurol. 2009;51:256–67.
35. Pinchefsky EF, Accogli A, Shevell MI, Saint-Martin C, Srour M. Developmental outcomes in children with congenital cerebellar malformations. Dev Med Child Neurol. 2018;61(3):350–8.
36. Frosk P, Arts HH, Philippe J, Gunn CS, Brown EL, Chodirker B, et al. A truncating mutation in CEP55 is the likely cause of MARCH, a novel syndrome affecting neuronal mitosis. J Med Genet. 2017;54:490–501.
37. Kanca O, Andrews JC, Lee PT, Patel C, Braddock SR, Slavotinek AM, et al. De novo variants in WDR37 are associated with epilepsy, colobomas, dysmorphism, developmental delay, intellectual disability, and cerebellar hypoplasia. Am J Hum Genet. 2019;105:413–24.
38. Zou Z, Huang L, Lin S, He Z, Zhu H, Zhang Y, et al. Prenatal diagnosis of posterior fossa anomalies: additional value of chromosomal microarray analysis in fetuses with cerebellar hypoplasia. Prenat Diagn. 2018;38:91–8.
39. Shaffer LG, Rosenfeld JA, Dabell MP, Coppinger J, Bandholz AM, Ellison JW, et al. Detection rates of clinically significant genomic alterations by microarray analysis for specific anomalies detected by ultrasound. Prenat Diagn. 2012;32:986–95.
40. D'Antonio F, Khalil A, Garel C, Pilu G, Rizzo G, Lerman-Sagie T, et al. Systematic review and meta-analysis of isolated posterior fossa malformations on prenatal ultrasound imaging (part 1): nomenclature, diagnostic accuracy and associated anomalies. Ultrasound Obstet Gynecol : the official journal of the International Society of Ultrasound in Obstetrics and Gynecology. 2016;47:690–7.
41. Shimbo H, Yokoi T, Aida N, Mizuno S, Suzumura H, Nagai J, et al. Haploinsufficiency of BCL11A associated with cerebellar abnormalities in 2p15p16.1 deletion syndrome. Mol Gen Genomic Med. 2017;5:429–37.
42. Spennato P, Mirone G, Nastro A, Buonocore MC, Ruggiero C, Trischitta V, et al. Hydrocephalus in Dandy-Walker malformation. Child's Nerv Syst : ChNS : official journal of the International Society for Pediatric Neurosurgery. 2011;27:1665–81.
43. Azab WA, Shohoud SA, Elmansoury TM, Salaheddin W, Nasim K, Parwez A. Blake's pouch cyst. Surg Neurol Int. 2014;5:112.
44. Murray JC, Johnson JA, Bird TD. Dandy-Walker malformation: etiologic heterogeneity and empiric recurrence risks. Clin Genet. 1985;28:272–83.
45. Aldinger KA, Lehmann OJ, Hudgins L, Chizhikov VV, Bassuk AG, Ades LC, et al. FOXC1 is required for normal cerebellar development and is a major contributor to chromosome 6p25.3 Dandy-Walker malformation. Nat Genet. 2009;41:1037–42.
46. Sowden JC. Molecular and developmental mechanisms of anterior segment dysgenesis. Eye (London, England). 2007;21:1310–8.
47. French CR, Seshadri S, Destefano AL, Fornage M, Arnold CR, Gage PJ, et al. Mutation of FOXC1 and PITX2 induces cerebral small-vessel disease. J Clin Invest. 2014;124:4877–81.
48. Ferraris A, Bernardini L, Sabolic Avramovska V, Zanni G, Loddo S, Sukarova-Angelovska E, et al. Dandy-Walker malformation and Wisconsin syndrome: novel cases add further insight into the genotype-phenotype correlations of 3q23q25 deletions. Orphanet J Rare Diseases. 2013;8:75.

49. Aruga J, Millen KJ. ZIC1 function in normal cerebellar development and human developmental pathology. Adv Exp Med Biol. 2018;1046:249–68.
50. McCormack WM Jr, Shen JJ, Curry SM, Berend SA, Kashork C, Pinar H, et al. Partial deletions of the long arm of chromosome 13 associated with holoprosencephaly and the Dandy-Walker malformation. Am J Med Genet. 2003;112(Part A 118a):384–9.
51. Darbro BW, Mahajan VB, Gakhar L, Skeie JM, Campbell E, Wu S, et al. Mutations in extracellular matrix genes NID1 and LAMC1 cause autosomal dominant Dandy-Walker malformation and occipital cephaloceles. Hum Mutat. 2013;34:1075–9.
52. Kolanczyk M, Krawitz P, Hecht J, Hupalowska A, Miaczynska M, Marschner K, et al. Missense variant in CCDC22 causes X-linked recessive intellectual disability with features of Ritscher-Schinzel/3C syndrome. Eur J Human Gen : EJHG. 2015;23:633–8.
53. Yang CA, Chou IC, Cho DY, Lin CY, Huang HY, Ho YC, et al. Whole exome sequencing in Dandy-Walker variant with intellectual disability reveals an activating CIP2A mutation as novel genetic cause. Neurogenetics. 2018;19:157–63.
54. Parisi M, and Glass I (1993). Joubert syndrome. In GeneReviews((R)), Adam M.P, Ardinger HH, Pagon, R.A. Wallace S.E, Bean LJH, Stephens K, and Amemiya A, eds. (Seattle (WA), University of Washington, Seattle. University of Washington, Seattle. GeneReviews is a registered trademark of the University of Washington, Seattle. All rights reserved.
55. Doherty D. Joubert syndrome: insights into brain development, cilium biology, and complex disease. Semin Pediatr Neurol. 2009;16:143–54.
56. Poretti A, Huisman TA, Scheer I, Boltshauser E. Joubert syndrome and related disorders: spectrum of neuroimaging findings in 75 patients. AJNR Am J Neuroradiol. 2011;32:1459–63.
57. Senocak EU, Oguz KK, Haliloglu G, Topcu M, Cila A. Structural abnormalities of the brain other than molar tooth sign in Joubert syndrome-related disorders. Diagn Interv Radiol. 2010;16:3–6.
58. Aldinger KA, Doherty D. The genetics of cerebellar malformations. Semin Fetal Neonatal Med. 2016;21:321–32.
59. Braun DA, Hildebrandt F. Ciliopathies. Cold Spring Harb Perspect Biol. 2017;9:a028191.
60. Guemez-Gamboa A, Coufal NG, Gleeson JG. Primary cilia in the developing and mature brain. Neuron. 2014;82:511–21.
61. Lancaster MA, Gopal DJ, Kim J, Saleem SN, Silhavy JL, Louie CM, et al. Defective Wnt-dependent cerebellar midline fusion in a mouse model of Joubert syndrome. Nat Med. 2011;17:726–31.
62. Aguilar A, Meunier A, Strehl L, Martinovic J, Bonniere M, Attie-Bitach T, et al. Analysis of human samples reveals impaired SHH-dependent cerebellar development in Joubert syndrome/Meckel syndrome. Proc Natl Acad Sci U S A. 2012;109:16,951–6.
63. Ishak GE, Dempsey JC, Shaw DW, Tully H, Adam MP, Sanchez-Lara PA, et al. Rhombencephalosynapsis: a hindbrain malformation associated with incomplete separation of midbrain and forebrain, hydrocephalus and a broad spectrum of severity. Brain J Neurol. 2012;135:1370–86.
64. Pasquier L, Marcorelles P, Loget P, Pelluard F, Carles D, Perez MJ, et al. Rhombencephalosynapsis and related anomalies: a neuropathological study of 40 fetal cases. Acta Neuropathol. 2009;117:185–200.
65. Tully HM, Dempsey JC, Ishak GE, Adam MP, Mink JW, Dobyns WB, et al. Persistent figure-eight and side-to-side head shaking is a marker for rhombencephalosynapsis. Mov Disorders: official journal of the Movement Disorder Society. 2013;28:2019–23.
66. Accogli A, Srour M. Teaching video neuroimages: figure 8 head-shaking stereotypy in rhombencephalosynapsis. Neurology. 2018;90:e1832–3.
67. Alter BP, Giri N. Thinking of VACTERL-H? Rule out Fanconi anemia according to PHENOS. Am J Med Genet A. 2016;170:1520–4.
68. Mak CCY, Doherty D, Lin AE, Vegas N, Cho MT, Viot G, et al. MN1 C-terminal truncation syndrome is a novel neurodevelopmental and craniofacial disorder with partial rhombencephalosynapsis. Brain J Neurol. 2020;143:55–68.
69. Aldinger KA, Dempsey JC, Tully HM, Grout ME, Mehaffey MG, Dobyns WB, et al. Rhombencephalosynapsis: fused cerebellum, confused geneticists. Am J Med Genet C: Semin Med Genet. 2018;178:432–9.
70. Barth PG, Majoie CB, Caan MW, Weterman MA, Kyllerman M, Smit LM, et al. Pontine tegmental cap dysplasia: a novel brain malformation with a defect in axonal guidance. Brain J Neurol. 2007;130:2258–66.
71. Jissendi-Tchofo P, Doherty D, McGillivray G, Hevner R, Shaw D, Ishak G, et al. Pontine tegmental cap dysplasia: MR imaging and diffusion tensor imaging features of impaired axonal navigation. AJNR Am J Neuroradiol. 2009;30:113–9.
72. Picker-Minh S, Hartenstein S, Proquitte H, Frohler S, Raile V, Kraemer N, et al. Pontine tegmental cap dysplasia in an extremely preterm infant and review of the literature. J Child Neurol. 2017;32:334–40.
73. Engle EC. Human genetic disorders of axon guidance. Cold Spring Harb Perspect Biol. 2010;2:a001784.
74. Poretti A, Denecke J, Miller DC, Schiffmann H, Buhk JH, Grange DK, et al. Brainstem disconnection: two additional patients and expansion of the phenotype. Neuropediatrics. 2015;46:139–44.
75. Barth PG, Aronica E, Fox S, Fluiter K, Weterman MAJ, Poretti A, et al. Deregulated expression of EZH2 in congenital brainstem disconnection. Neuropathol Appl Neurobiol. 2017;43:358–65.
76. Zaki MS, Saleem SN, Dobyns WB, Barkovich AJ, Bartsch H, Dale AM, et al. Diencephalic-mesencephalic junction dysplasia: a novel recessive brain malformation. Brain J Neurol. 2012;135:2416–27.
77. Severino M, Tortora D, Pistorio A, Ramenghi LA, Napoli F, Mancardi MM, et al. Expanding the spectrum of congenital anomalies of the diencephalic-mesencephalic junction. Neuroradiology. 2016;58:33–44.
78. Guemez-Gamboa A, Caglayan AO, Stanley V, Gregor A, Zaki MS, Saleem SN, et al. Loss of protocadherin-12 leads to diencephalic-mesencephalic junction dysplasia syndrome. Ann Neurol. 2018;84:638–47.
79. Aran A, Rosenfeld N, Jaron R, Renbaum P, Zuckerman S, Fridman H, et al. Loss of function of PCDH12 underlies recessive microcephaly mimicking intrauterine infection. Neurology. 2016;86:2016–24.
80. Rampon C, Prandini MH, Bouillot S, Pointu H, Tillet E, Frank R, et al. Protocadherin 12 (VE-cadherin 2) is expressed in endothelial, trophoblast, and mesangial cells. Exp Cell Res. 2005;302:48–60.
81. Moog U, Jones MC, Bird LM, Dobyns WB. Oculocerebrocutaneous syndrome: the brain malformation defines a core phenotype. J Med Genet. 2005;42:913–21.
82. Moog U, Dobyns WB. An update on oculocerebrocutaneous (Delleman-Oorthuys) syndrome. Am J Med Genet C: Semin Med Genet. 2018;178:414–22.
83. van Dijk T, Baas F, Barth PG, Poll-The BT. What's new in pontocerebellar hypoplasia? An update on genes and subtypes. Orphanet J Rare Diseases. 2018;13:92.
84. Ognjenovic J, Simonovic M. Human aminoacyl-tRNA synthetases in diseases of the nervous system. RNA Biol. 2018;15:623–34.
85. Namavar Y, Barth PG, Kasher PR, van Ruissen F, Brockmann K, Bernert G, et al. Clinical, neuroradiological and genetic findings in pontocerebellar hypoplasia. Brain J Neurol. 2011;134:143–56.

86. Akizu N, Cantagrel V, Schroth J, Cai N, Vaux K, McCloskey D, et al. AMPD2 regulates GTP synthesis and is mutated in a potentially treatable neurodegenerative brainstem disorder. Cell. 2013;154:505–17.
87. Severino M, Zara F, Rossi A, Striano P. Teaching neuroimages: figure of 8: the clue to the diagnosis of AMPD2 pontocerebellar hypoplasia (PCH9). Neurology. 2017;89:e172–3.
88. Renbaum P, Kellerman E, Jaron R, Geiger D, Segel R, Lee M, et al. Spinal muscular atrophy with pontocerebellar hypoplasia is caused by a mutation in the VRK1 gene. Am J Hum Genet. 2009;85:281–9.
89. Wan J, Yourshaw M, Mamsa H, Rudnik-Schoneborn S, Menezes MP, Hong JE, et al. Mutations in the RNA exosome component gene EXOSC3 cause pontocerebellar hypoplasia and spinal motor neuron degeneration. Nat Genet. 2012;44:704–8.
90. Boczonadi V, Muller JS, Pyle A, Munkley J, Dor T, Quartararo J, et al. EXOSC8 mutations alter mRNA metabolism and cause hypomyelination with spinal muscular atrophy and cerebellar hypoplasia. Nat Commun. 2014;5:4287.
91. Wan J, Steffen J, Yourshaw M, Mamsa H, Andersen E, Rudnik-Schoneborn S, et al. Loss of function of SLC25A46 causes lethal congenital pontocerebellar hypoplasia. Brain J Neurol. 2016;139:2877–90.
92. Ivanov I, Atkinson D, Litvinenko I, Angelova L, Andonova S, Mumdjiev H, et al. Pontocerebellar hypoplasia type 1 for the neuropediatrician: genotype-phenotype correlations and diagnostic guidelines based on new cases and overview of the literature. Eur J Paediatr Neurol : EJPN : official journal of the European Paediatric Neurology Society. 2018;22:674–81.
93. Agamy O, Ben Zeev B, Lev D, Marcus B, Fine D, Su D, et al. Mutations disrupting selenocysteine formation cause progressive cerebello-cerebral atrophy. Am J Hum Genet. 2010;87:538–44.
94. Pavlidou E, Salpietro V, Phadke R, Hargreaves IP, Batten L, McElreavy K, et al. Pontocerebellar hypoplasia type 2D and optic nerve atrophy further expand the spectrum associated with selenoprotein biosynthesis deficiency. Eur J Paediatr Neurol : EJPN : official journal of the European Paediatric Neurology Society. 2016;20:483–8.
95. Feinstein M, Flusser H, Lerman-Sagie T, Ben-Zeev B, Lev D, Agamy O, et al. VPS53 mutations cause progressive cerebello-cerebral atrophy type 2 (PCCA2). J Med Genet. 2014;51:303–8.
96. Ekert K, Groeschel S, Sanchez-Albisua I, Frolich S, Dieckmann A, Engel C, et al. Brain morphometry in pontocerebellar hypoplasia type 2. Orphanet J Rare Diseases. 2016;11:100.
97. Bierhals T, Korenke GC, Uyanik G, Kutsche K. Pontocerebellar hypoplasia type 2 and TSEN2: review of the literature and two novel mutations. Eur J Med Gen. 2013;56:325–30.
98. Breuss MW, Sultan T, James KN, Rosti RO, Scott E, Musaev D, et al. Autosomal-recessive mutations in the tRNA splicing endonuclease subunit TSEN15 cause pontocerebellar hypoplasia and progressive microcephaly. Am J Hum Genet. 2016;99:228–35.
99. Namavar Y, Chitayat D, Barth PG, van Ruissen F, de Wissel MB, Poll-The BT, et al. TSEN54 mutations cause pontocerebellar hypoplasia type 5. Eur J Human Gen : EJHG. 2011;19:724–6.
100. Ahmed MY, Chioza BA, Rajab A, Schmitz-Abe K, Al-Khayat A, Al-Turki S, et al. Loss of PCLO function underlies pontocerebellar hypoplasia type III. Neurology. 2015;84:1745–50.
101. Cassandrini D, Cilio MR, Bianchi M, Doimo M, Balestri M, Tessa A, et al. Pontocerebellar hypoplasia type 6 caused by mutations in RARS2: definition of the clinical spectrum and molecular findings in five patients. J Inherit Metab Dis. 2013;36:43–53.
102. Lardelli RM, Schaffer AE, Eggens VR, Zaki MS, Grainger S, Sathe S, et al. Biallelic mutations in the 3′ exonuclease TOE1 cause pontocerebellar hypoplasia and uncover a role in snRNA processing. Nat Genet. 2017;49:457–64.
103. Mochida GH, Ganesh VS, de Michelena MI, Dias H, Atabay KD, Kathrein KL, et al. CHMP1A encodes an essential regulator of BMI1-INK4A in cerebellar development. Nat Genet. 2012;44:1260–4.
104. Kortum F, Jamra RA, Alawi M, Berry SA, Borck G, Helbig KL, et al. Clinical and genetic spectrum of AMPD2-related pontocerebellar hypoplasia type 9. Eur J Human Gen: EJHG. 2018;26:695–708.
105. Schaffer AE, Eggens VR, Caglayan AO, Reuter MS, Scott E, Coufal NG, et al. CLP1 founder mutation links tRNA splicing and maturation to cerebellar development and neurodegeneration. Cell. 2014;157:651–63.
106. Ivanova EL, Mau-Them FT, Riazuddin S, Kahrizi K, Laugel V, Schaefer E, et al. Homozygous truncating variants in TBC1D23 cause pontocerebellar hypoplasia and alter cortical development. Am J Hum Genet. 2017;101:428–40.
107. Marin-Valencia I, Gerondopoulos A, Zaki MS, Ben-Omran T, Almureikhi M, Demir E, et al. Homozygous mutations in TBC1D23 lead to a non-degenerative form of pontocerebellar hypoplasia. Am J Hum Genet. 2017;101:441–50.
108. Chi H, Yang X, Kingsley PD, O'Keefe RJ, Puzas JE, Rosier RN, et al. Targeted deletion of Minpp1 provides new insight into the activity of multiple inositol polyphosphate phosphatase in vivo. Mol Cell Biol. 2000;20:6496–507.
109. Appelhof B, Wagner M, Hoefele J, Heinze A, Roser T, Koch-Hogrebe M, Roosendaal SD, Dehghani M, Mehrjardi MYV, Torti E, et al. (2020). Pontocerebellar hypoplasia due to bi-allelic variants in MINPP1. Eur J Hum Genet.
110. Wojcik MH, Okada K, Prabhu SP, Nowakowski DW, Ramsey K, Balak C, Rangasamy S, Brownstein CA, Schmitz-Abe K, Cohen JS, et al. (2018). De novo variant in KIF26B is associated with pontocerebellar hypoplasia with infantile spinal muscular atrophy. Am J Med Gen Part A.
111. Accogli A, Russell L, Sebire G, Riviere JB, St-Onge J., Addour-Boudrahem N, Laporte AD, Rouleau GA, Saint-Martin C, and Srour M (2019). Pathogenic variants in AIMP1 cause pontocerebellar hypoplasia. Neurogenetics.
112. Najm J, Horn D, Wimplinger I, Golden JA, Chizhikov VV, Sudi J, et al. Mutations of CASK cause an X-linked brain malformation phenotype with microcephaly and hypoplasia of the brainstem and cerebellum. Nat Genet. 2008;40:1065–7.
113. Moog U, Kutsche K, Kortum F, Chilian B, Bierhals T, Apeshiotis N, et al. Phenotypic spectrum associated with CASK loss-of-function mutations. J Med Genet. 2011;48:741–51.
114. Burglen L, Chantot-Bastaraud S, Garel C, Milh M, Touraine R, Zanni G, et al. Spectrum of pontocerebellar hypoplasia in 13 girls and boys with CASK mutations: confirmation of a recognizable phenotype and first description of a male mosaic patient. Orphanet J Rare Diseases. 2012;7:18.
115. Hayashi S, Uehara DT, Tanimoto K, Mizuno S, Chinen Y, Fukumura S, et al. Comprehensive investigation of CASK mutations and other genetic etiologies in 41 patients with intellectual disability and microcephaly with pontine and cerebellar hypoplasia (MICPCH). PLoS One. 2017;12:e0181791.
116. Moog U, Bierhals T, Brand K, Bautsch J, Biskup S, Brune T, et al. Phenotypic and molecular insights into CASK-related disorders in males. Orphanet J Rare Diseases. 2015;10:44.
117. Sparks SE, Quijano-Roy S, Harper A, Rutkowski A, Gordon E, Hoffman EP, and Pegoraro E (1993). Congenital muscular dystrophy overview. In GeneReviews((R)), M.P. Adam, H.H. Ardinger, R.A. Pagon, S.E. Wallace, L.J.H. Bean, K. Stephens, and A. Amemiya, eds. (Seattle (WA), University of Washington, Seattle. University of Washington, Seattle. GeneReviews is a registered trademark of the University of Washington, Seattle. All rights reserved.

118. Sparks SE, and Krasnewich, D.M. (1993). PMM2-CDG (CDG-Ia). In GeneReviews((R)), M.P. Adam, H.H. Ardinger, R.A. Pagon, S.E. Wallace, L.J.H. Bean, K. Stephens, andA. Amemiya, eds. (Seattle (WA), University of Washington, Seattle University of Washington, Seattle. GeneReviews is a registered trademark of the University of Washington, Seattle. All rights reserved.
119. Feraco P, Mirabelli-Badenier M, Severino M, Alpigiani MG, Di Rocco M, Biancheri R, et al. The shrunken, bright cerebellum: a characteristic MRI finding in congenital disorders of glycosylation type 1a. AJNR Am J Neuroradiol. 2012;33:2062–7.
120. Cantagrel V, Lefeber DJ, Ng BG, Guan Z, Silhavy JL, Bielas SL, et al. SRD5A3 is required for converting polyprenol to dolichol and is mutated in a congenital glycosylation disorder. Cell. 2010;142:203–17.
121. Morava E, Wevers RA, Cantagrel V, Hoefsloot LH, Al-Gazali L, Schoots J, et al. A novel cerebello-ocular syndrome with abnormal glycosylation due to abnormalities in dolichol metabolism. Brain J Neurol. 2010;133:3210–20.
122. Barone R, Fiumara A, Jaeken J. Congenital disorders of glycosylation with emphasis on cerebellar involvement. Semin Neurol. 2014;34:357–66.
123. Sun L, Zhao Y, Zhou K, Freeze HH, Zhang YW, Xu H. Insufficient ER-stress response causes selective mouse cerebellar granule cell degeneration resembling that seen in congenital disorders of glycosylation. Molecular brain. 2013;6:52.
124. Heywood WE, Bliss E, Mills P, Yuzugulen J, Carreno G, Clayton PT, et al. Global serum glycoform profiling for the investigation of dystroglycanopathies & congenital disorders of glycosylation. Mol Gen Metab Rep. 2016;7:55–62.
125. Bernard G, Chouery E, Putorti ML, Tetreault M, Takanohashi A, Carosso G, et al. Mutations of POLR3A encoding a catalytic subunit of RNA polymerase Pol III cause a recessive hypomyelinating leukodystrophy. Am J Hum Genet. 2011;89:415–23.
126. Tetreault M, Choquet K, Orcesi S, Tonduti D, Balottin U, Teichmann M, et al. Recessive mutations in POLR3B, encoding the second largest subunit of Pol III, cause a rare hypomyelinating leukodystrophy. Am J Hum Genet. 2011;89:652–5.
127. Borck G, Hog F, Dentici ML, Tan PL, Sowada N, Medeira A, et al. BRF1 mutations alter RNA polymerase III-dependent transcription and cause neurodevelopmental anomalies. Genome Res. 2015;25:155–66.
128. Jee YH, Sowada N, Markello TC, Rezvani I, Borck G, Baron J. BRF1 mutations in a family with growth failure, markedly delayed bone age, and central nervous system anomalies. Clin Genet. 2017;91:739–47.
129. Fu, Y., Tvrdik, P., Makki, N., Paxinos, G., and Watson, C. (2011). Precerebellar cell groups in the hindbrain of the mouse defined by retrograde tracing and correlated with cumulative Wnt1-cre genetic labeling. Cerebellum (London, England) 10, 570–584.
130. Wurst W, Prakash N. Wnt1-regulated genetic networks in midbrain dopaminergic neuron development. J Mol Cell Biol. 2014;6:34–41.
131. McMahon AP, Bradley A. The Wnt-1 (int-1) proto-oncogene is required for development of a large region of the mouse brain. Cell. 1990;62:1073–85.
132. Thomas KR, Musci TS, Neumann PE, Capecchi MR. Swaying is a mutant allele of the proto-oncogene Wnt-1. Cell. 1991;67:969–76.
133. Bahi-Buisson N, Poirier K, Fourniol F, Saillour Y, Valence S, Lebrun N, et al. The wide spectrum of tubulinopathies: what are the key features for the diagnosis? Brain J Neurol. 2014;137:1676–700.
134. Tischfield MA, Engle EC. Distinct alpha- and beta-tubulin isotypes are required for the positioning, differentiation and survival of neurons: new support for the 'multi-tubulin' hypothesis. Biosci Rep. 2010;30:319–30.
135. Oegema R, Cushion TD, Phelps IG, Chung SK, Dempsey JC, Collins S, et al. Recognizable cerebellar dysplasia associated with mutations in multiple tubulin genes. Hum Mol Genet. 2015;24:5313–25.
136. Romaniello R, Arrigoni F, Panzeri E, Poretti A, Micalizzi A, Citterio A, et al. Tubulin-related cerebellar dysplasia: definition of a distinct pattern of cerebellar malformation. Eur Radiol. 2017;27:5080–92.
137. Romaniello R, Arrigoni F, Fry AE, Bassi MT, Rees MI, Borgatti R, et al. Tubulin genes and malformations of cortical development. Eur J Med Gen. 2018;61:744–54.
138. Bahi-Buisson N, and Cavallin M (1993). Tubulinopathies overview. In GeneReviews((R)), M.P. Adam, H.H. Ardinger, R.A. Pagon, S.E. Wallace, L.J.H. Bean, K. Stephens, andA. Amemiya, eds. (Seattle (WA), University of Washington, Seattle University of Washington, Seattle. GeneReviews is a registered trademark of the University of Washington, Seattle. All rights reserved.
139. Scala M, Torella A, Severino M, Morana G, Castello R, Accogli A, et al. Three de novo DDX3X variants associated with distinctive brain developmental abnormalities and brain tumor in intellectually disabled females. Eur J Human Gen: EJHG. 2019;27:1254–9.
140. Chen HH, Yu HI, Tarn WY. DDX3 modulates neurite development via translationally activating an RNA regulon involved in Rac1 activation. J Neurosci Off J Soc Neurosci. 2016;36:9792–804.
141. Tivodar S, Kalemaki K, Kounoupa Z, Vidaki M, Theodorakis K, Denaxa M, et al. Rac-GTPases regulate microtubule stability and axon growth of cortical GABAergic interneurons. Cereb Cortex (New York, NY: 1991). 2015;25:2370–82.
142. Honda T, Kobayashi K, Mikoshiba K, Nakajima K. Regulation of cortical neuron migration by the Reelin signaling pathway. Neurochem Res. 2011;36:1270–9.
143. Miyata T, Ono Y, Okamoto M, Masaoka M, Sakakibara A, Kawaguchi A, et al. Migration, early axonogenesis, and Reelin-dependent layer-forming behavior of early/posterior-born Purkinje cells in the developing mouse lateral cerebellum. Neural Dev. 2010;5:23.
144. Valence S, Garel C, Barth M, Toutain A, Paris C, Amsallem D, et al. RELN and VLDLR mutations underlie two distinguishable clinico-radiological phenotypes. Clin Genet. 2016;90:545–9.
145. Clement E, Mercuri E, Godfrey C, Smith J, Robb S, Kinali M, et al. Brain involvement in muscular dystrophies with defective dystroglycan glycosylation. Ann Neurol. 2008;64:573–82.
146. Godfrey C, Clement E, Mein R, Brockington M, Smith J, Talim B, et al. Refining genotype phenotype correlations in muscular dystrophies with defective glycosylation of dystroglycan. Brain J Neurol. 2007;130:2725–35.
147. Devisme L, Bouchet C, Gonzales M, Alanio E, Bazin A, Bessieres B, et al. Cobblestone lissencephaly: neuropathological subtypes and correlations with genes of dystroglycanopathies. Brain J Neurol. 2012;135:469–82.
148. Bahi-Buisson N, Poirier K, Boddaert N, Fallet-Bianco C, Specchio N, Bertini E, et al. GPR56-related bilateral frontoparietal polymicrogyria: further evidence for an overlap with the cobblestone complex. Brain J Neurol. 2010;133:3194–209.
149. Vandervore L, Stouffs K, Tanyalcin I, Vanderhasselt T, Roelens F, Holder-Espinasse M, et al. Bi-allelic variants in COL3A1 encoding the ligand to GPR56 are associated with cobblestone-like cortical malformation, white matter changes and cerebellar cysts. J Med Genet. 2017;54:432–40.
150. Horn D, Siebert E, Seidel U, Rost I, Mayer K, Abou Jamra R, et al. Biallelic COL3A1 mutations result in a clinical spectrum of

specific structural brain anomalies and connective tissue abnormalities. Am J Med Genet A. 2017;173:2534–8.
151. Luo R, Jeong SJ, Jin Z, Strokes N, Li S, Piao X. G protein-coupled receptor 56 and collagen III, a receptor-ligand pair, regulates cortical development and lamination. Proc Natl Acad Sci U S A. 2011;108:12,925–30.
152. Luo R, Jeong SJ, Yang A, Wen M, Saslowsky DE, Lencer WI, et al. Mechanism for adhesion G protein-coupled receptor GPR56-mediated RhoA activation induced by collagen III stimulation. PLoS One. 2014;9:e100043.
153. Magen D, Ofir A, Berger L, Goldsher D, Eran A, Katib N, et al. Autosomal recessive lissencephaly with cerebellar hypoplasia is associated with a loss-of-function mutation in CDK5. Hum Genet. 2015;134:305–14.
154. Xu B, Kumazawa A, Kobayashi S, Hisanaga SI, Inoue T, Ohshima T. Cdk5 activity is required for Purkinje cell dendritic growth in cell-autonomous and non-cell-autonomous manners. Dev Neurobiol. 2017;77:1175–87.
155. Shinmyo Y, Terashita Y, Dinh Duong TA, Horiike T, Kawasumi M, Hosomichi K, et al. Folding of the cerebral cortex requires Cdk5 in upper-layer neurons in gyrencephalic mammals. Cell Rep. 2017;20:2131–43.
156. Pagnamenta AT, Howard MF, Wisniewski E, Popitsch N, Knight SJ, Keays DA, et al. Germline recessive mutations in PI4KA are associated with perisylvian polymicrogyria, cerebellar hypoplasia and arthrogryposis. Hum Mol Genet. 2015;24:3732–41.
157. Cappuccio G, Pinelli M, Torella A, Vitiello G, D'Amico A, Alagia M, et al. An extremely severe phenotype attributed to WDR81 nonsense mutations. Ann Neurol. 2017;82:650–1.
158. Cavallin M, Rujano MA, Bednarek N, Medina-Cano D, Bernabe Gelot A, Drunat S, et al. WDR81 mutations cause extreme microcephaly and impair mitotic progression in human fibroblasts and Drosophila neural stem cells. Brain J Neurol. 2017;140:2597–609.
159. Traka M, Millen KJ, Collins D, Elbaz B, Kidd GJ, Gomez CM, et al. WDR81 is necessary for purkinje and photoreceptor cell survival. J Neurosci Off J Soc Neurosci. 2013;33:6834–44.
160. Gueneau L, Fish RJ, Shamseldin HE, Voisin N, Tran Mau-Them F, Preiksaitiene E, et al. KIAA1109 variants are associated with a severe disorder of brain development and arthrogryposis. Am J Hum Genet. 2018;102:116–32.
161. Dobyns WB, Aldinger KA, Ishak GE, Mirzaa GM, Timms AE, Grout ME, et al. MACF1 mutations encoding highly conserved zinc-binding residues of the GAR domain cause defects in neuronal migration and axon guidance. Am J Hum Genet. 2018;103:1009–21.
162. Tripathy R, Leca I, van Dijk T, Weiss J, van Bon BW, Sergaki MC, et al. Mutations in MAST1 cause mega-corpus-callosum syndrome with cerebellar hypoplasia and cortical malformations. Neuron. 2018;100:1354–1368.e1355.
163. Micalizzi A, Poretti A, Romani M, Ginevrino M, Mazza T, Aiello C, et al. Clinical, neuroradiological and molecular characterization of cerebellar dysplasia with cysts (Poretti-Boltshauser syndrome). Eur J Human Gen: EJHG. 2016;24:1262–7.
164. Boltshauser E, Scheer I, Huisman TA, Poretti A. Cerebellar cysts in children: a pattern recognition approach. Cerebellum (London, England). 2015;14:308–16.
165. Doherty D, Chudley AE, Coghlan G, Ishak GE, Innes AM, Lemire EG, et al. GPSM2 mutations cause the brain malformations and hearing loss in Chudley-McCullough syndrome. Am J Hum Genet. 2012;90:1088–93.
166. Mauriac SA, Hien YE, Bird JE, Carvalho SD, Peyroutou R, Lee SC, et al. Defective Gpsm2/Galphai3 signalling disrupts stereocilia development and growth cone actin dynamics in Chudley-McCullough syndrome. Nat Commun. 2017;8:14,907.
167. Olson HE, Jean-Marcais N, Yang E, Heron D, Tatton-Brown K, van der Zwaag PA, et al. A recurrent de novo PACS2 heterozygous missense variant causes neonatal-onset developmental epileptic encephalopathy, facial dysmorphism, and cerebellar dysgenesis. Am J Hum Genet. 2018;102:995–1007.